TRANSICIONES de FASE CUÁNTICAS
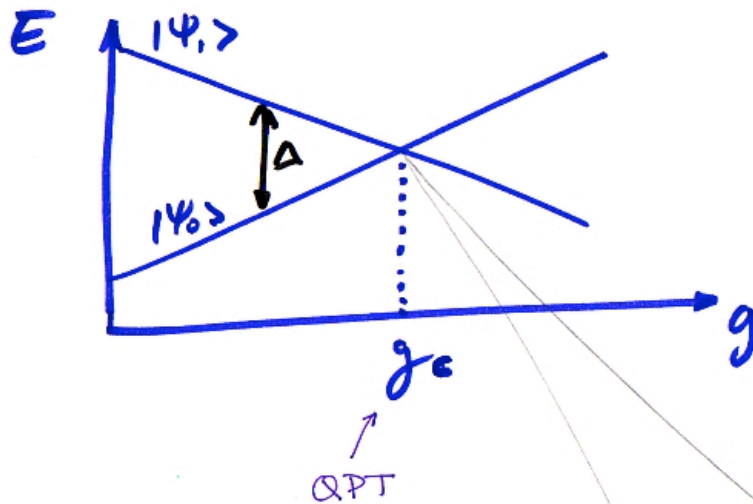
TRANSICIONES a $T=0$
DEBIDAS A LA VARIACIÓN DE UN PARÁMETRO (H, P, x, ...)
NO- TÉRMICO

Ph. Tr: (Classical)

- Papel esencial en la NATURALEZA
- "Cualquier" sistema físico tiene Ph. Tr. (U, H_2O ...)
  "termodinámico"

- Ocurren como variaciones de un parámetro de control

- $T \neq 0$: ORDEN MACROSCÓPICO vs. FLUCTUACIONES TÉRMICAS

- $T = 0$: Sólo $\exists$ FLUCTUACIONES CUÁNTICAS

Física de Bajas Temperaturas - Transiciones de Fase

$$\mathcal{H} = \mathcal{H}_0 + g\,\mathcal{H}_1$$

g: parámetro de control
$(H, P, E, x \dots)$

$$\mathcal{H}\,|\Psi_i\rangle = E_i\,|\Psi_i\rangle$$
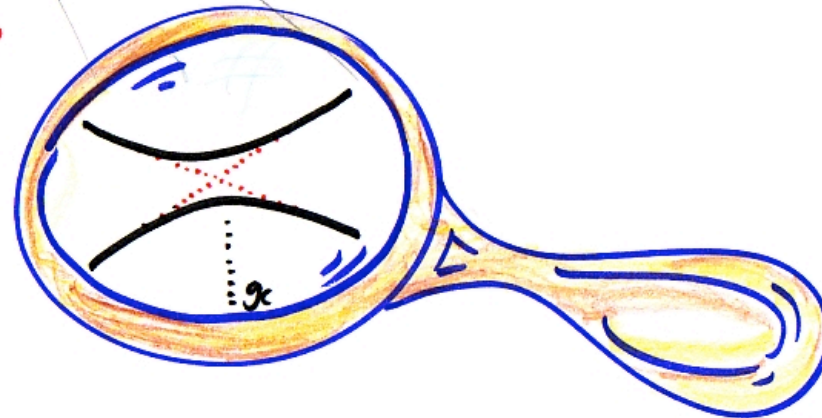
$$\Delta \sim J\,|g - g_c|^{z\nu}$$

Escala de Energías

0 en QPT

exponente crítico

E

$|\Psi_1\rangle$

Δ

$|\Psi_0\rangle$

g_c

g

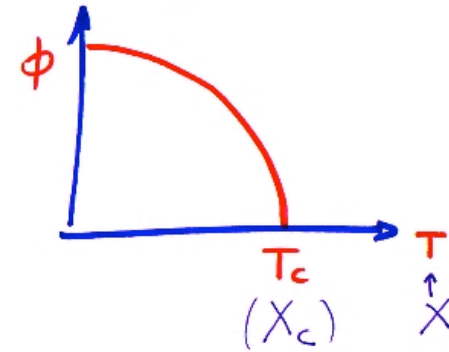QPT

"Avoided level crossing"

LA QPT VIENE ACOMPAÑADA
DE UN CAMBIO CUALITATIVO
EN LAS CORRELACIONES
DEL ESTADO FUNDAMENTAL

TRANSICIONES CONTINUAS

→ Order parameter

- $T > T_c \Rightarrow \langle \phi \rangle_T = 0$

  pero las fluctuaciones $\delta\phi \neq 0$, en gral.

- CERCA de T_c la LONGITUD de CORRELACIÓN ξ

  (l. característica de las $\delta\phi$) DIVERGE:

$$\xi \propto |t|^{-\nu} \qquad t = \frac{|T-T_c|}{T_c}$$

- $\exists$ un TIEMPO DE CORRELACIÓN (τ_c) ~ Tiempo típico de relajación.

$$\tau_c \propto \xi^z \propto |t|^{-\nu z}$$

$z \equiv$ exponente crítico dinámico

(graph: ϕ vs T, curve from ϕ axis to T_c (X_c), X)

Q.M. cerca del punto crítico.

2 aspectos

QM puede ser fundamental para entender la existencia de la fase ordenada (o ambas); e.g.:

- SUPERCONDUCTIVIDAD
- SUPERFLUIDEZ
- ...

¿ES la Q.M. relevante en el comportamiento crítico (asintótico)?
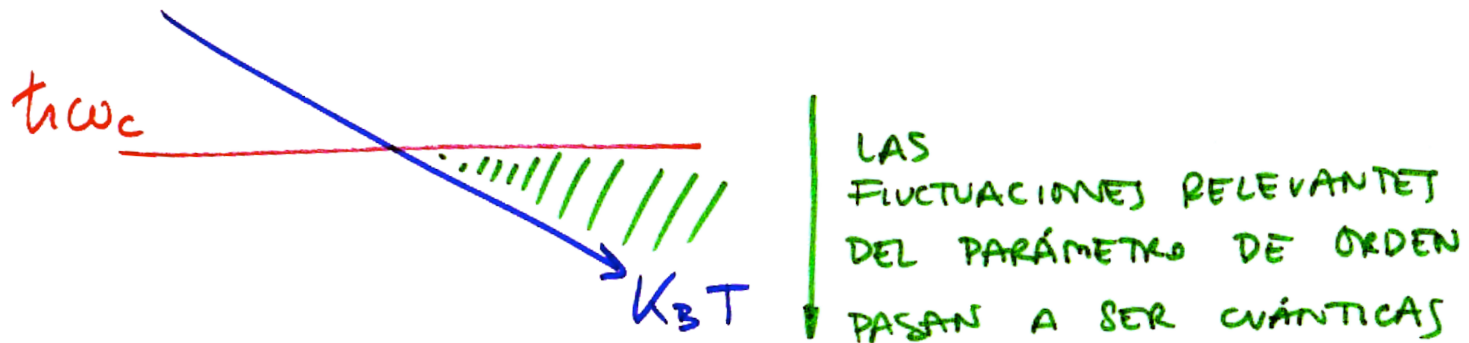
$$\tau_c \sim |t|^{-\nu z}$$

$$\hbar \omega_c \longrightarrow k_B T$$

$$\hbar \omega_c \sim |t|^{\nu z}$$

Física de Bajas Temperaturas - Transiciones de Fase

$$\hbar \omega_c \gtrsim K_B T \longrightarrow \text{QM relevante}$$

$$\hbar \omega_c \ll K_B T \longrightarrow \text{Classical description.}$$

$\hbar \omega_c$

$K_B T$

LAS FLUCTUACIONES RELEVANTES DEL PARÁMETRO DE ORDEN PASAN A SER CUÁNTICAS

pero

$$|t| = \frac{|T - T_c|}{T_c} < T_c^{1/\nu z}$$

$y \quad \hbar \omega_c \sim |t|^{\nu z}$

suficientemente CERCA de T_c ; $\boxed{\hbar \omega_c \ll K_B T}$ si T_c es finito

$\forall \; T_c \neq 0 \Rightarrow$ Ph. Tr. CLÁSICAS

• Si T_c es finita ...

① LAS FLUCTUACIONES CLASICAS DOMINAN LA TRANSICIÓN DE FASE, AUNQUE "SUFICIENTEMENTE CERCA" de T_c PUEDE QUERER DECIR "MUY CERCA!!" SI T_c ES MUY BAJA O LA DINAMICA LO REQUIERE ...

DA IGUAL: "ASINTOTICAMENTE", LA TR. ES CLÁSICA

② SI $T_c = 0$ ∄ FLUCTUACIONES CLASICAS ⇒ Q.P.T.

③ EL PARAMETRO DE CONTROL DEL ORDEN ES "NO-TÉRMICO"

④ DEPENDIENDO DE SI ∃ ORDEN A $T \neq 0$ O NO → 2 DIAGRAMAS de FASE

1D ≡ CADENA ISING

2D - XY → KOSTERITZ-THOULESS

ISING - 2D
FERROMAGNETO REAL
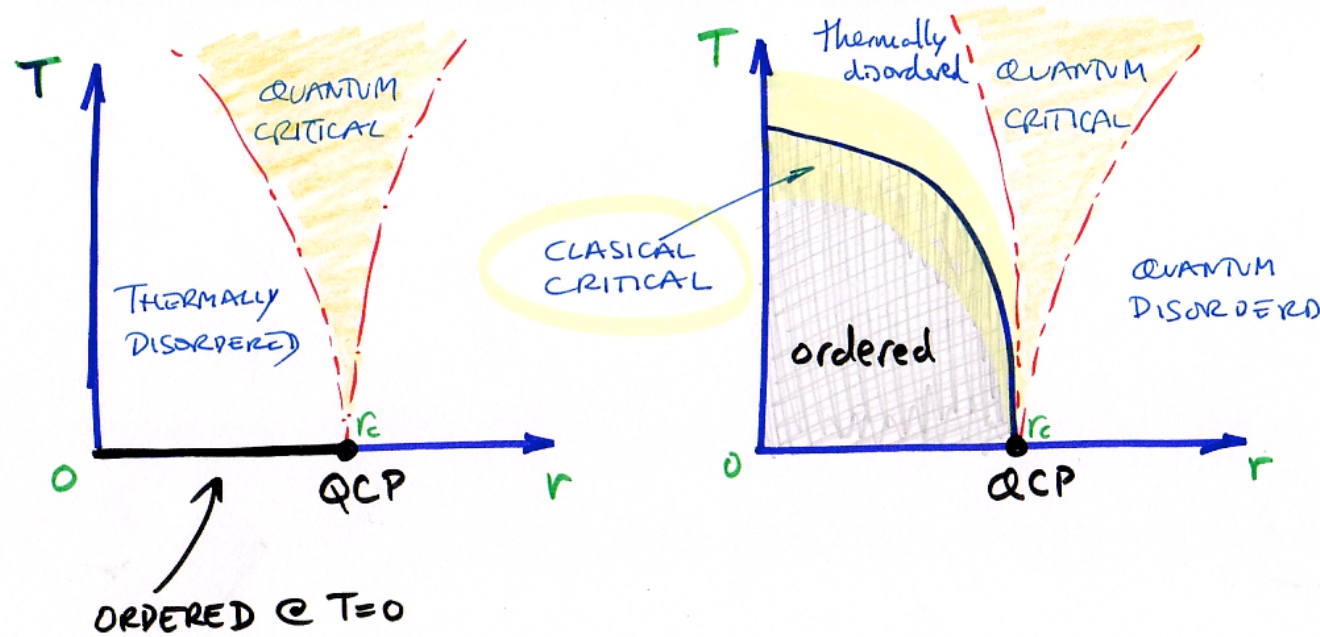DOPED $La_2Cu O_4$
⋮

④ DEPENDIENDO DE SI ∃ ORDEN A T≠0 O NO ⟶ 2 DIAGRAMAS de FASE

ORDERED @ T=0

QUÉ HAY EN LA REGIÓN CRÍTICA CUÁNTICA?

- LA FISICA ESTA CONTROLADA POR LAS EXCITACIONES TÉRMICAS DEL ESTADO FUNDAMENTAL CUÁNTICO
(Las excitaciones no son las habituales, las "leyes de potencias" no son las habituales, Comportamiento de líquido no-de-Fermi ...)

PARÁMETROS NO-TERMICOS EN Q.P.T.

- $x \equiv$ "Composición" $Ce\,Cu_{6-x}\,Au_x$

- $P \equiv$ PRESIÓN

- $H \equiv$ CAMPO MAGNÉTICO

Ejemplo "típico": $LiHoF_4$ ($T_c = 1.53\,K$ @ $H=0$)

model system
Ising under field

$$\mathcal{H} = \sum_{i,j}^{N} J_{ij}\,\sigma_i^z\,\sigma_j^z - \Gamma \sum_i^N \sigma_i^x$$

$\sigma \equiv$ Pauli matrices
$J_{ij} \equiv$ exchange cte.
$\Gamma \equiv$ transversal field

Quantum Critical Behavior for a Model Magnet
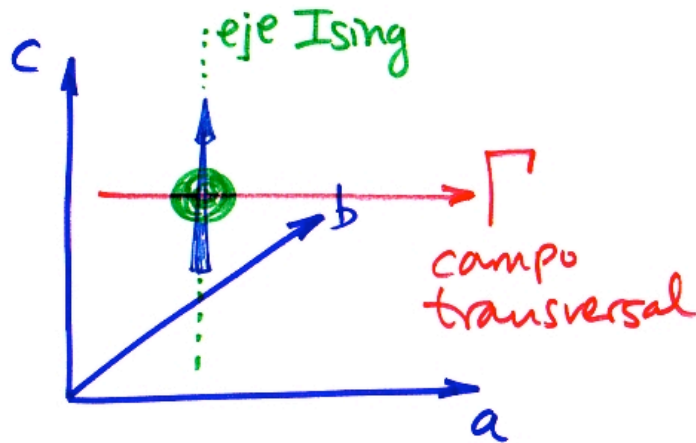
D. Bitko and T. F. Rosenbaum

The James Franck Institute and Department of Physics, The University of Chicago, Chicago, Illinois 60637
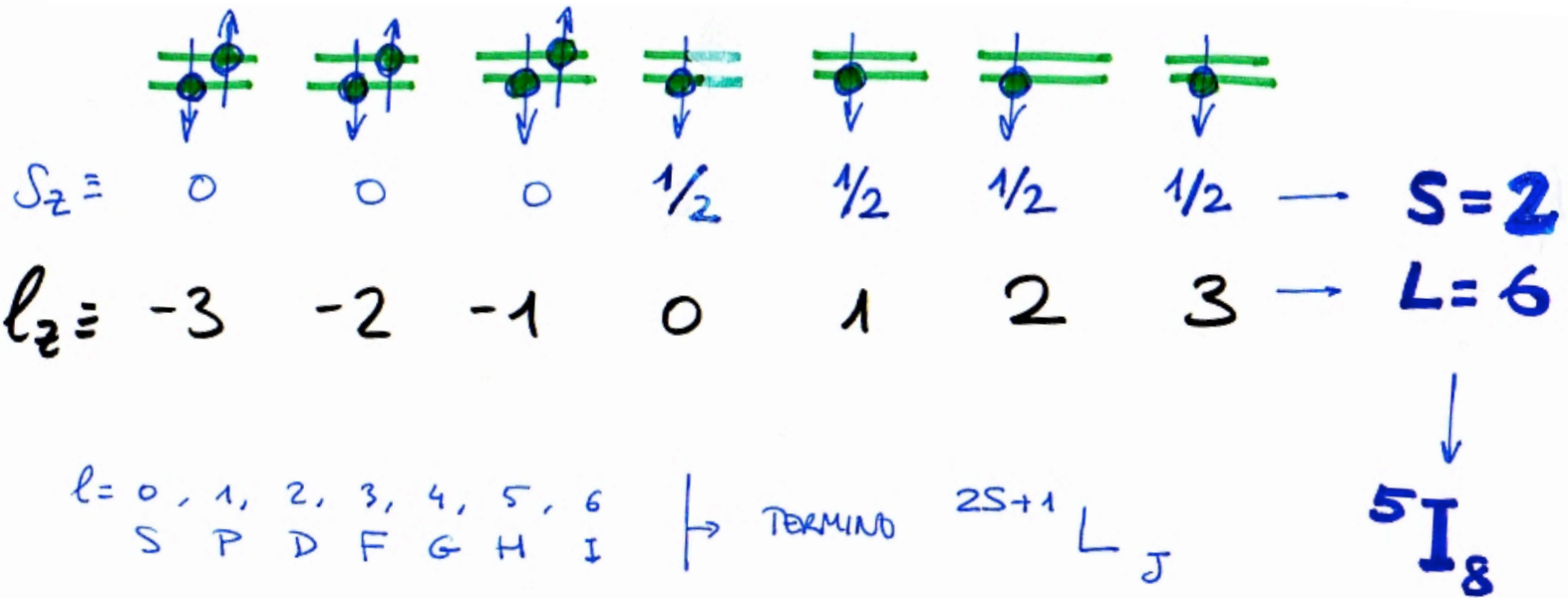
G. Aeppli

NEC Research Institute, 4 Independence Way, Princeton, New Jersey 08540
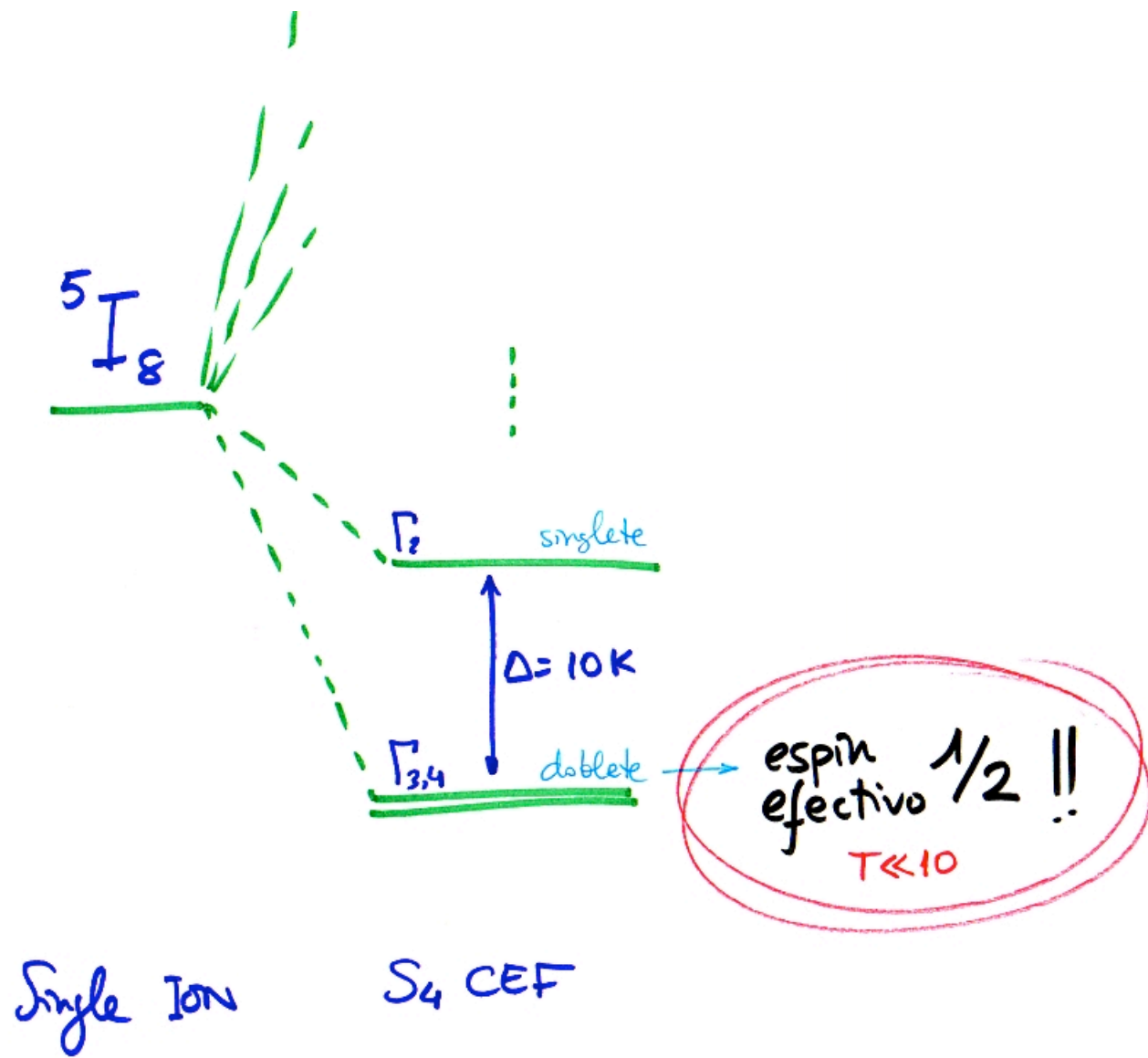(Received 18 March 1996)

The classical, thermally driven transition in the dipolar-coupled Ising ferromagnet LiHoF$_4$ ($T_c = 1.53$ K) can be converted into a quantum transition driven by a transverse magnetic field H_t at $T = 0$. The transverse field, applied perpendicular to the Ising axis, introduces channels for quantum relaxation, thereby depressing T_c. We have determined the phase diagram in the H_t-T plane via magnetic susceptibility measurements. The critical exponent, $\gamma = 1$, has a mean-field value in both the classical and quantum limits. A solution of the full mean-field Hamiltonian using the known LiHoF$_4$ crystal-field wave functions, including nuclear hyperfine terms, accurately matches experiment.   [S0031-9007(96)00753-3]
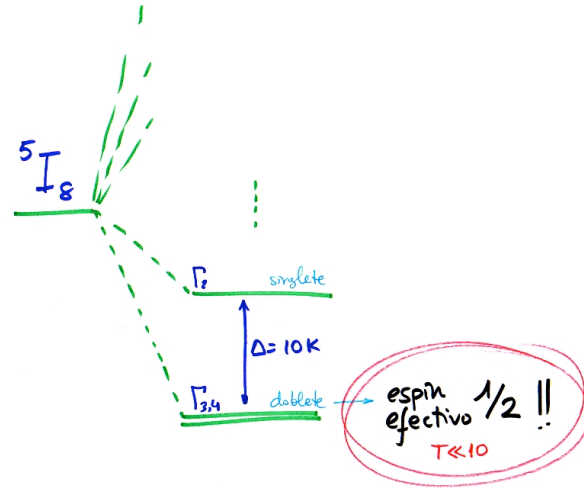
eje Ising

c

b

Γ

campo transversal

a

Ho^{3+} : $4f^{10}$

$S_z =$ 0   0   0   ½   ½   ½   ½ $\longrightarrow$ $S = 2$

$l_z =$ -3   -2   -1   0   1   2   3 $\longrightarrow$ $L = 6$

$l =$ 0 , 1 , 2 , 3 , 4 , 5 , 6
   S   P   D   F   G   H   I $\longmapsto$ TÉRMINO $^{2S+1}L_J$

$^5I_8$

$$5\underset{8}{\mathbf{I}}$$

single
ion

$^5I_8$

$\Gamma_?$ singlete

$\Delta = 10K$

$\Gamma_{3,4}$ doblete → espin efectivo $^1/_2$!!

$T \ll 10$

• ISING ?? Depende del **detalle** "fino" del CEF

$$|\phi_i\rangle = \sum_{i=-\frac{15}{2}}^{15/2} a_i \,|6,\tfrac{3}{2},\tfrac{15}{2},i\rangle \quad ; \quad \sum_{i=-\frac{15}{2}}^{15/2} |a_i|^2 = 1$$

← los a_is determinan

$$\overleftrightarrow{g} \equiv \begin{bmatrix} g_{xx} & g_{xy} & g_{xz} \\ g_{yx} & g_{yy} & g_{yz} \\ g_{zx} & g_{zy} & g_{zz} \end{bmatrix}$$

Critical behavior of the magnetic susceptibility of the uniaxial ferromagnet LiHoF₄

P. Beauvillain and J.-P. Renard

*Institut d'Electronique Fondamentale, Laboratoire associé au Centre National de la Recherche Scientifique
Bâtiment 220, Université Paris-Sud, 91405 Orsay Cédex, France*

I. Laursen

Department of Electrophysics, Building 322, The Technical University of Denmark, DK-2800, Lyngby, Denmark

P. J. Walker

Clarendon Laboratory, Parks Road, Oxford, United Kingdom
(Received 21 February 1978).

The magnetic susceptibility of two LiHoF₄ single crystals has been measured in the range 1.2−4.2 K. Ferromagnetic order occurs at $T_c = 1.527$ K. Above 2.5 K, the susceptibilities parallel and perpendicular to the fourfold c axis are well interpreted by the molecular-field approximation, taking into account the ground state and the first excited state of Ho^{3+} in the crystal field of S_4 symmetry. The experimental results are consistent with $g_{\parallel} = 13.95$ and $g_{\perp} = 0$ for the ground state. The dipolar contribution to the magnetic interaction is about three times larger than the exchange one. Near T_c, the parallel susceptibility is well described by the classical law with logarithmic corrections theoretically predicted by Larkin and Khmel'mitskii for the uniaxial dipolar ferromagnet or by a power law with a critical-exponent value $\gamma = 1.05$ rather close to 1. The upper limit of the critical region is $(T_{max} - T_c)/T_c = 1.1 \times 10^{-2}$.
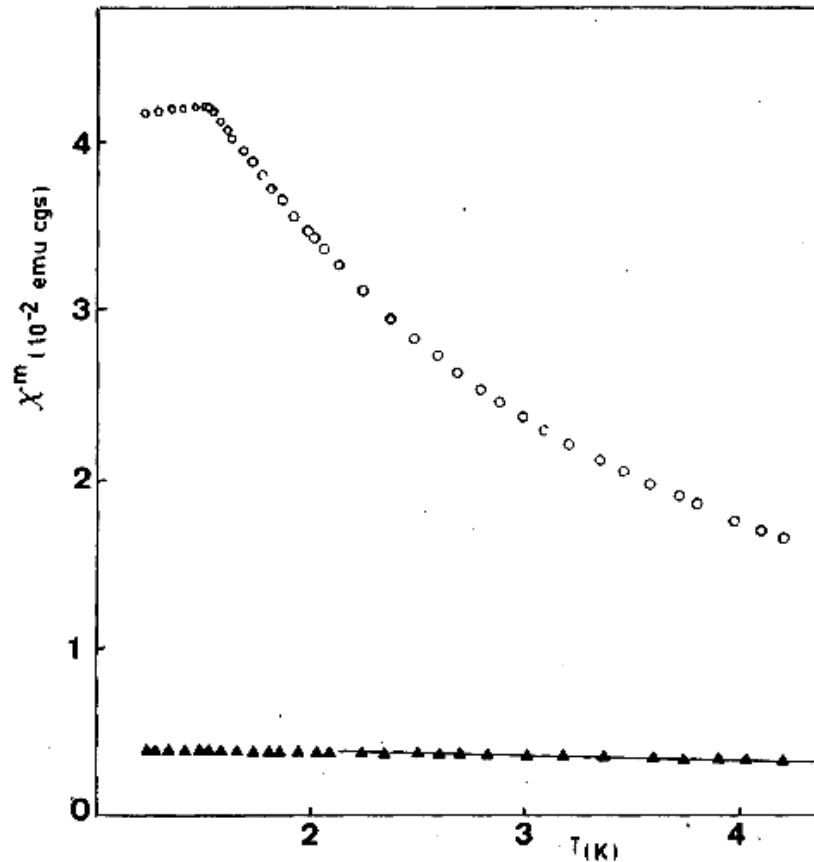
FIG. 1. Experimental parallel susceptibility per gram $\chi_{\parallel}^{m}$ (open circles) and perpendicular susceptibility per gram $\chi_{\perp}^{m}$ (black triangles) vs temperature for the spherical sample. The solid line represents the approximate theoretical law, for $e^{-E_1/kT} \ll 1$: $\chi_{\perp}^{m} = (n\mu_{B}^{2}/4k)(B + Ce^{-E_1/kT})$, with $B = 9.98$, $C = 11.3$, and $E_1/k = 10.4$ K.
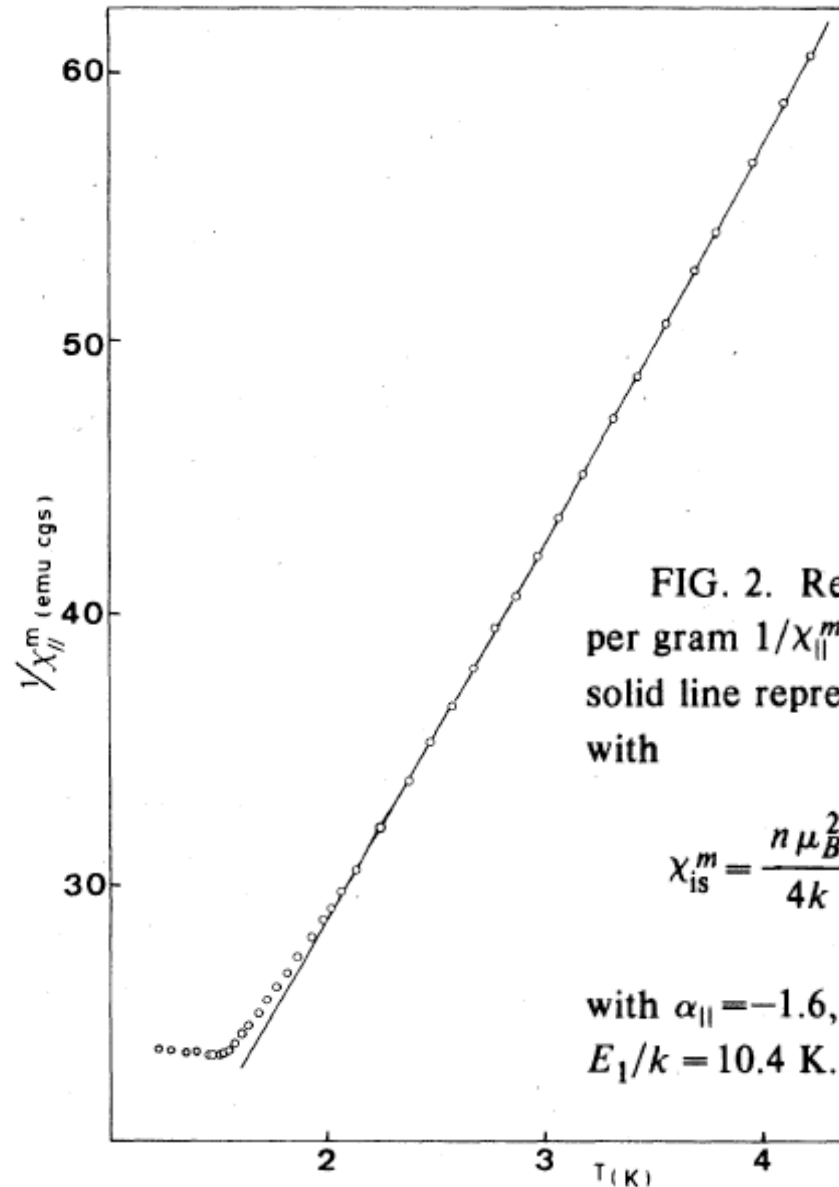
FIG. 2. Reciprocal experimental parallel susceptibility per gram $1/\chi_{\|}^m$ vs temperature for a spherical sample. The solid line represents the theoretical curve $1/\chi_{\|}^m = 1/\chi_{is}^m - \alpha_{\|}$ with

$$\chi_{is}^m = \frac{n\mu_B^2}{4k}\left[\frac{(g_{\|}^0)^2 T^{-1} + a_{\|}^0 + a_{\|}^1 e^{-E_1/kT}}{1 + 0.5 e^{-E_1/kT}}\right]$$

with $\alpha_{\|} = -1.6$, $g_{\|}^0 = 13.95$, $a_{\|}^0 = 0.25$, $a_{\|}^1 = 3.3$, and $E_1/k = 10.4$ K.

$$\chi^m_{isol} = \frac{n\mu_B^2}{4K_B} \cdot \frac{g^0_{//} T^{-1} + a^0_{//} + a^1_{//} e^{-E_1/K_B T}}{1 + \frac{1}{2} e^{-E_1/K_B T}}$$

GIROMAGNETIC RATIO

VAN VLECK

$$g^0_{//} = 13.95 \quad (X)$$
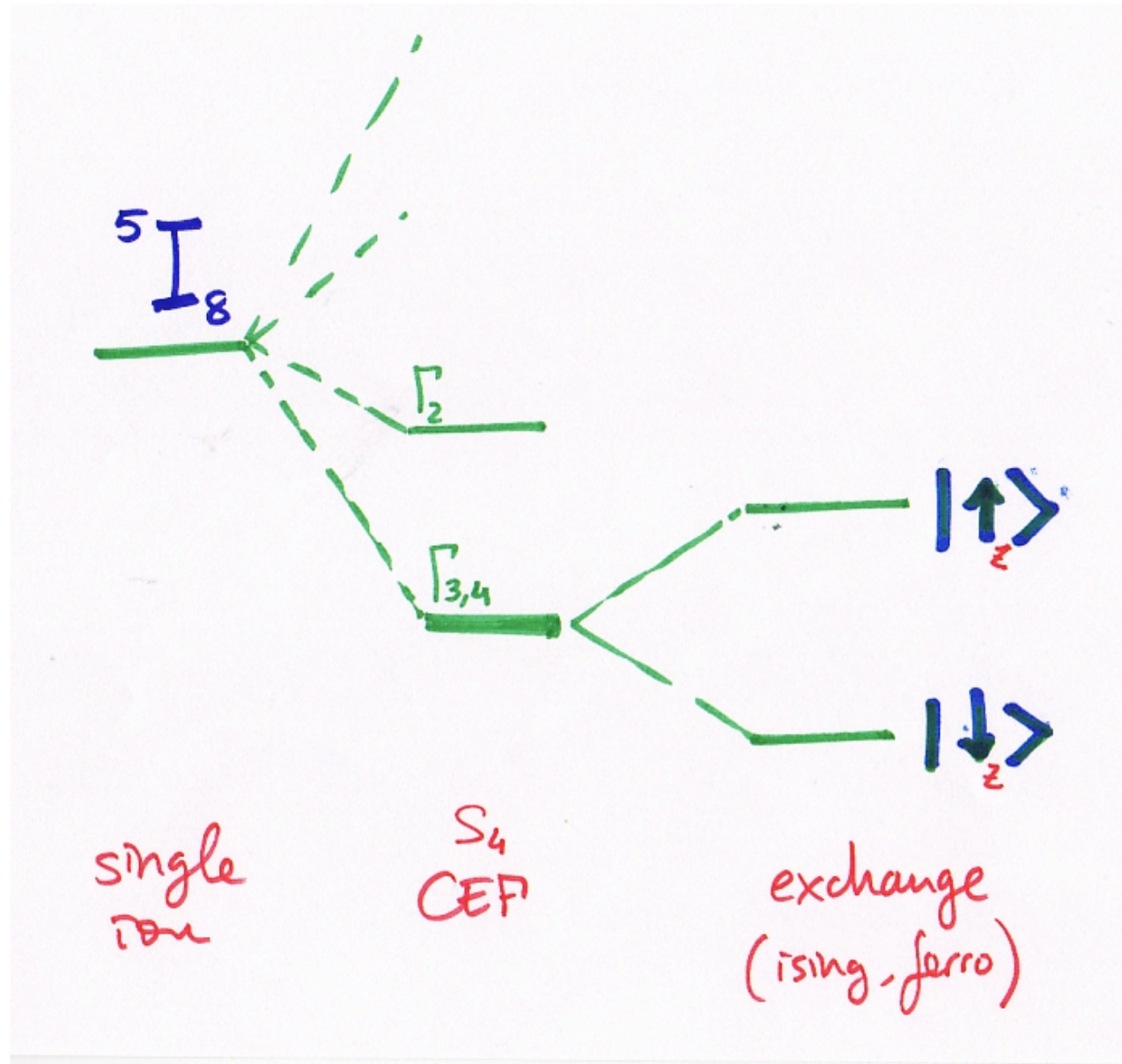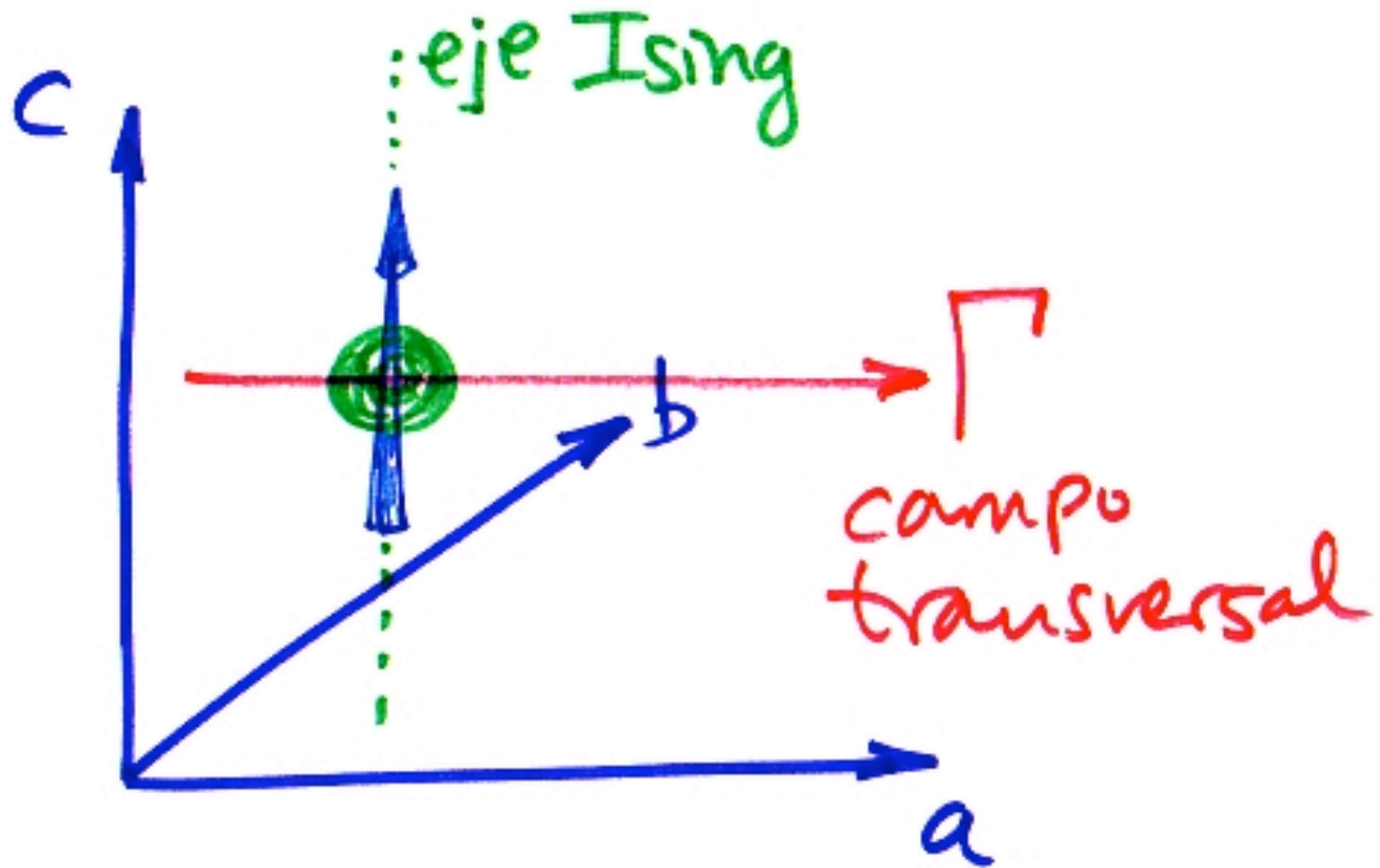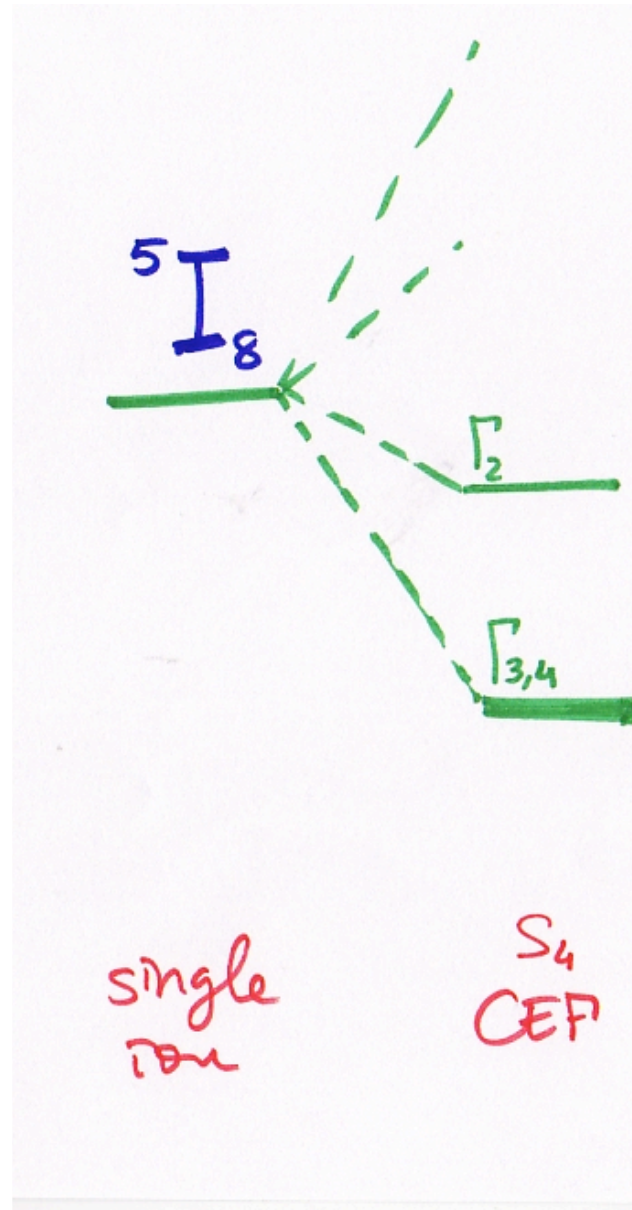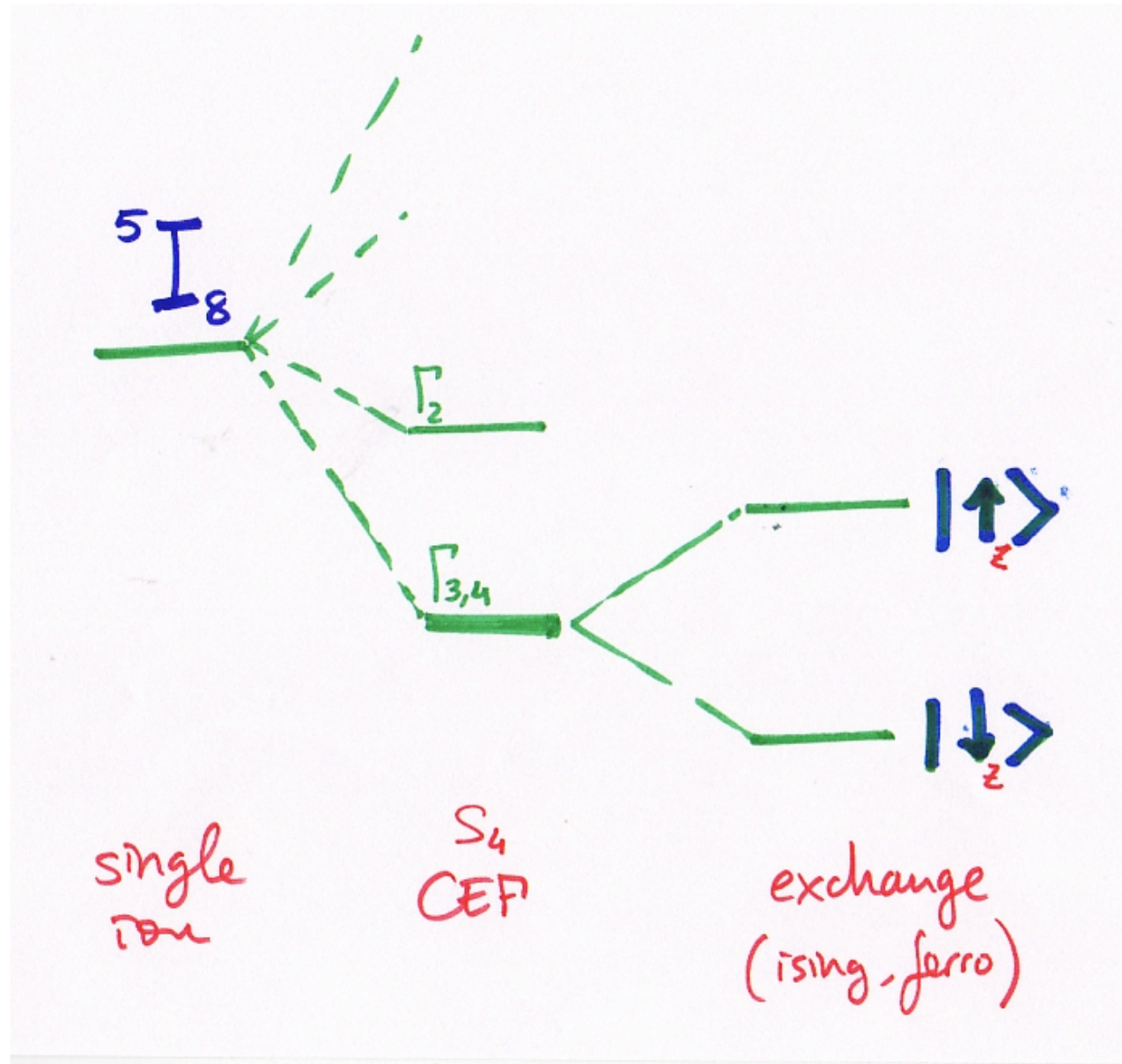
$$g^0_{//} = 14.1(2) \quad E.P.R$$
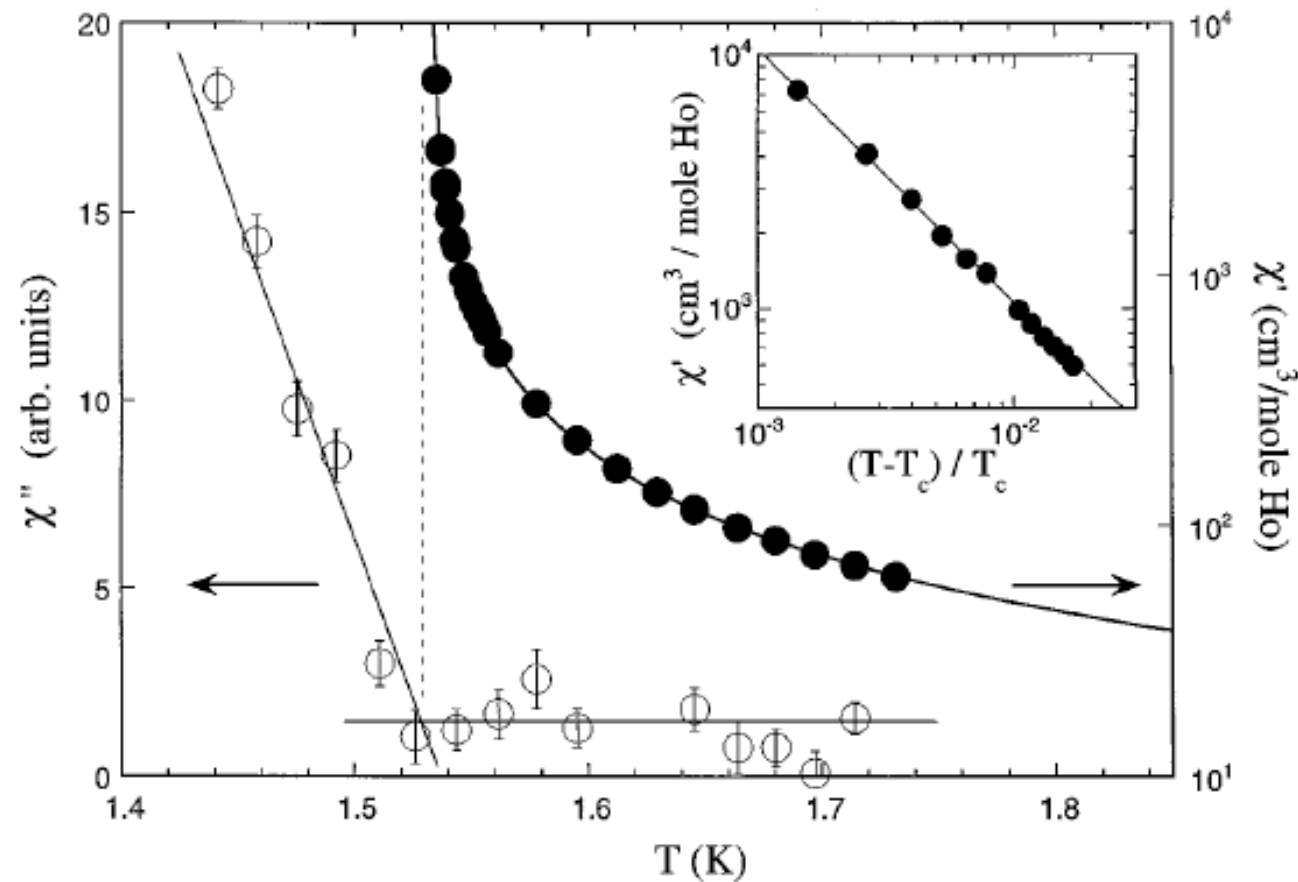
FIG. 1. Divergence of the real part of the magnetic suscepti-bility (filled circles) and sharp increase in the imaginary part (open circles) at the thermally driven ferromagnetic transition in $LiHoF_4$. Inset: Mean-field critical behavior with $\chi' \propto t^{-\gamma}$ and best-fit value $\gamma = 1.00 \pm 0.09$ (line).
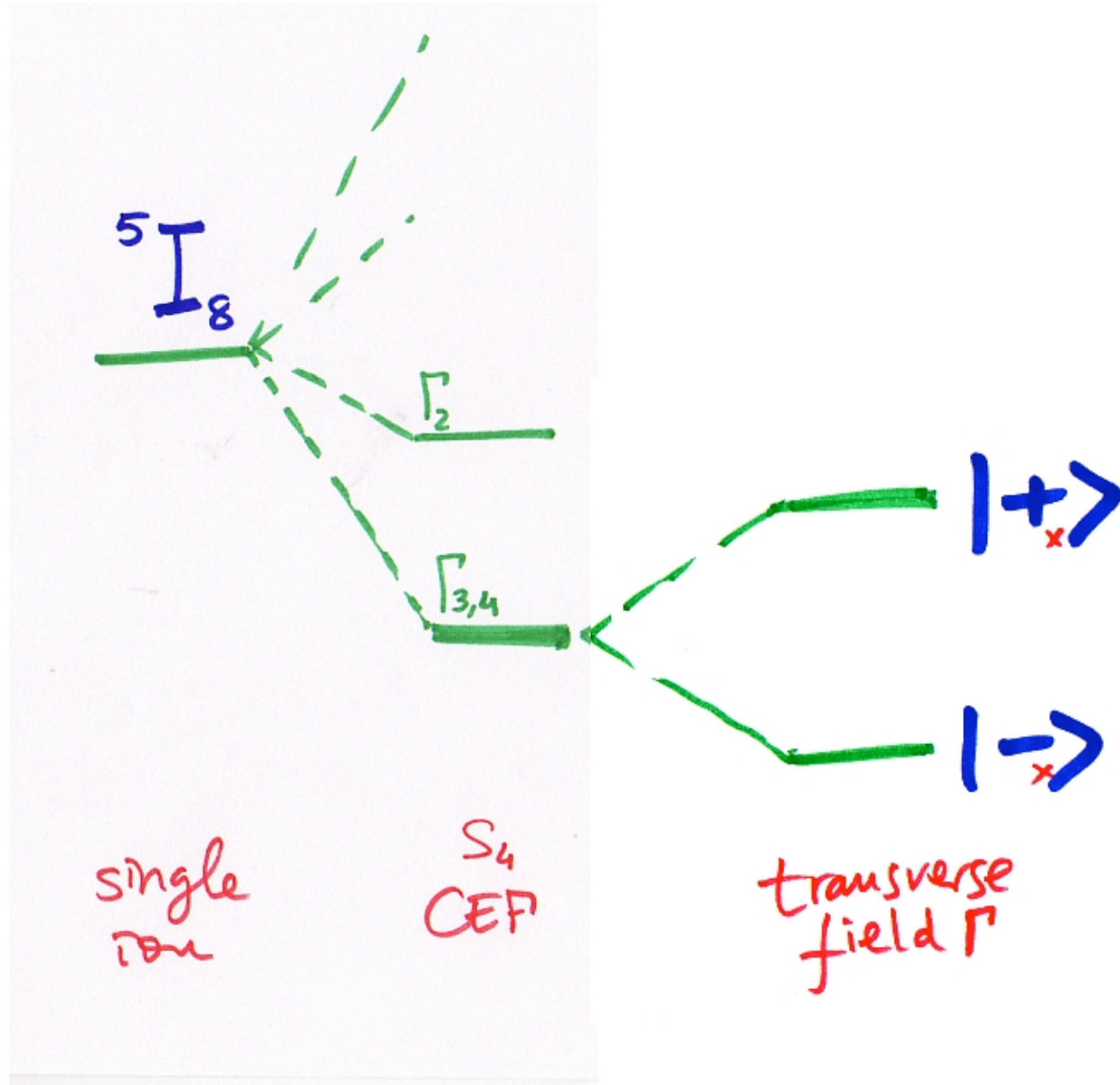
Física de Bajas Temperaturas - Transiciones de Fase

$$|\pm\rangle = \frac{1}{\sqrt{2}} \left(|\uparrow_z\rangle \pm |\downarrow_z\rangle \right)$$

Transición (*de fase cuántica*) de

Orden Clásico Ferromagnético

a Desorden Cuántico !!

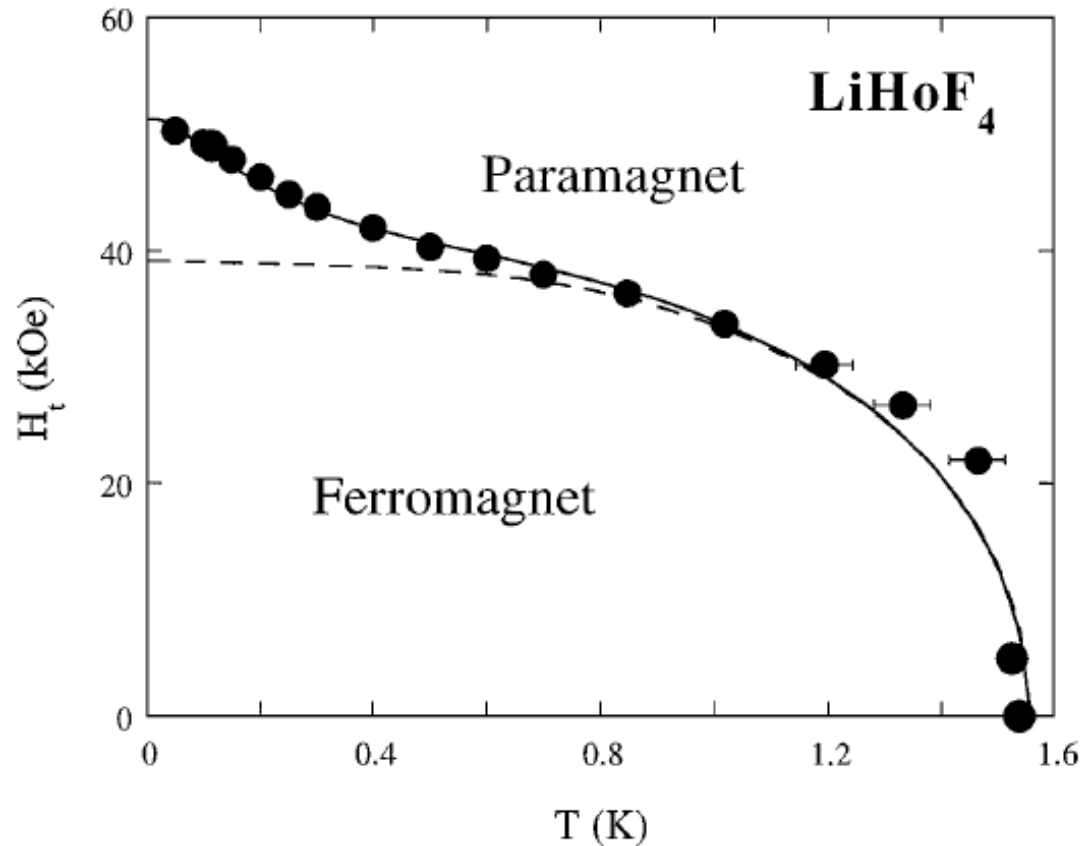Física de Bajas Temperaturas - Transiciones de Fase

FIG. 3. Experimental phase boundary (filled circles) for the ferromagnetic transition in the transverse field-temperature plane. Dashed line is a mean-field theory including only the electronic spin degrees of freedom; solid line is a full mean-field theory incorporating the nuclear hyperfine interaction [Eq. (2)]. Both theories have the same two fitting parameters.
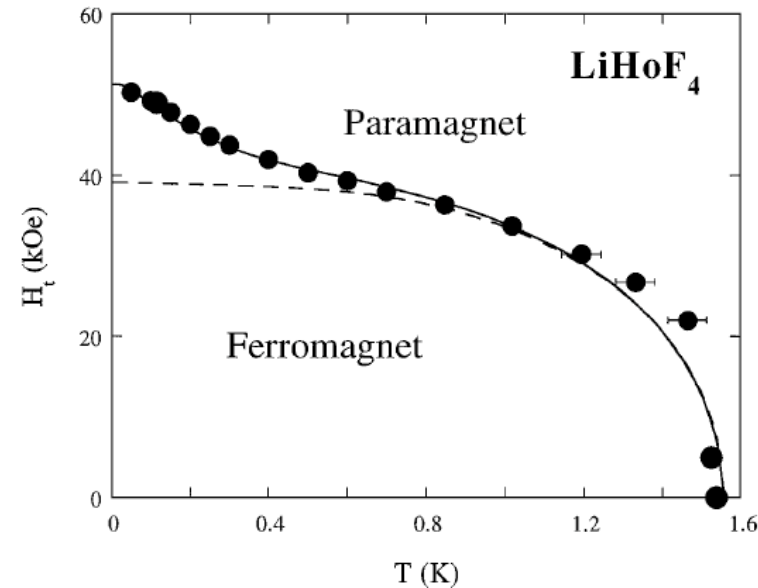
$T > 0.6 K$ $\qquad \coth\left(\Gamma/2\kappa T_c\right) = J/\Gamma$ ---

ising ferro; transverse field

$T < 0.6 K$ $\qquad$ nuclear hyperfine interaction needed

$$\mathcal{H} = V_c - g_\perp \mu_B \Gamma \vec{J}_x + A\left(\vec{I}\cdot\vec{J}\right) - 2J\langle\vec{J}_z\rangle\vec{J}_z$$

$I = 7/2$

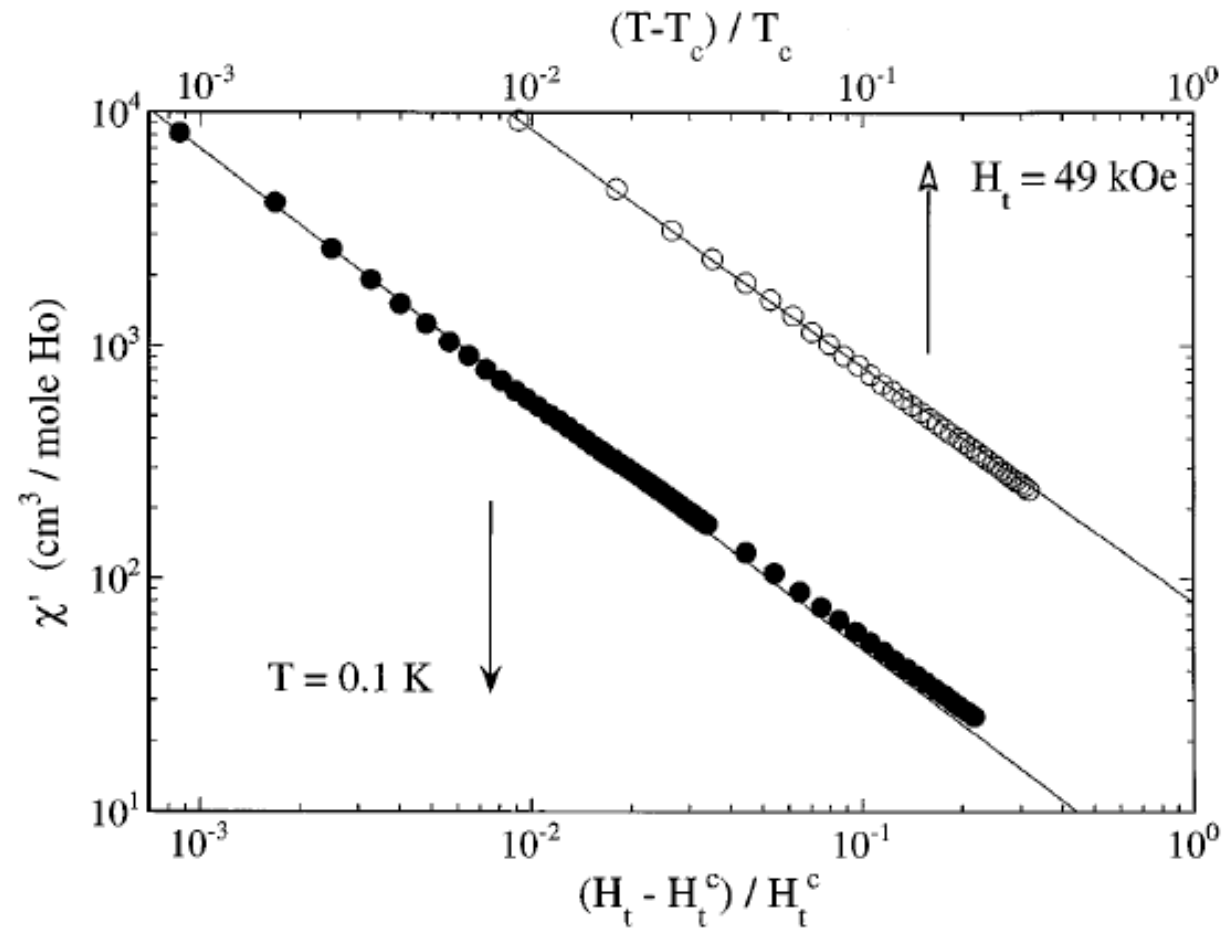Física de Bajas Temperaturas - Transiciones de Fase

FIG. 2. Mean-field critical behavior of the magnetic suscep-
tibility in the $T \rightarrow 0$ limit as functions of reduced tempera-
ture (open circles, $T_c = 0.114$ K, $H_t = 49.0$ kOe) and reduced
transverse field (filled circles, $H_t^c = 49.3$ kOe, $T = 0.100$ K).

We find $\gamma = 1$ within error bars at all temperatures studied, down to the lowest temperature probed, $T = 0.050$ K or 3% of $T_c(H_t = 0)$. Hence, we conclude that the critical behavior at the quantum ferromagnetic transition in $LiHoF_4$ retains its mean-field character. This observation verifies the theoretical prediction [11] that the $T = 0$ critical exponents of a d-dimensional Ising model in transverse field are equivalent to those of a $(d + 1)$-diemensional Ising model in zero transverse field. Studies
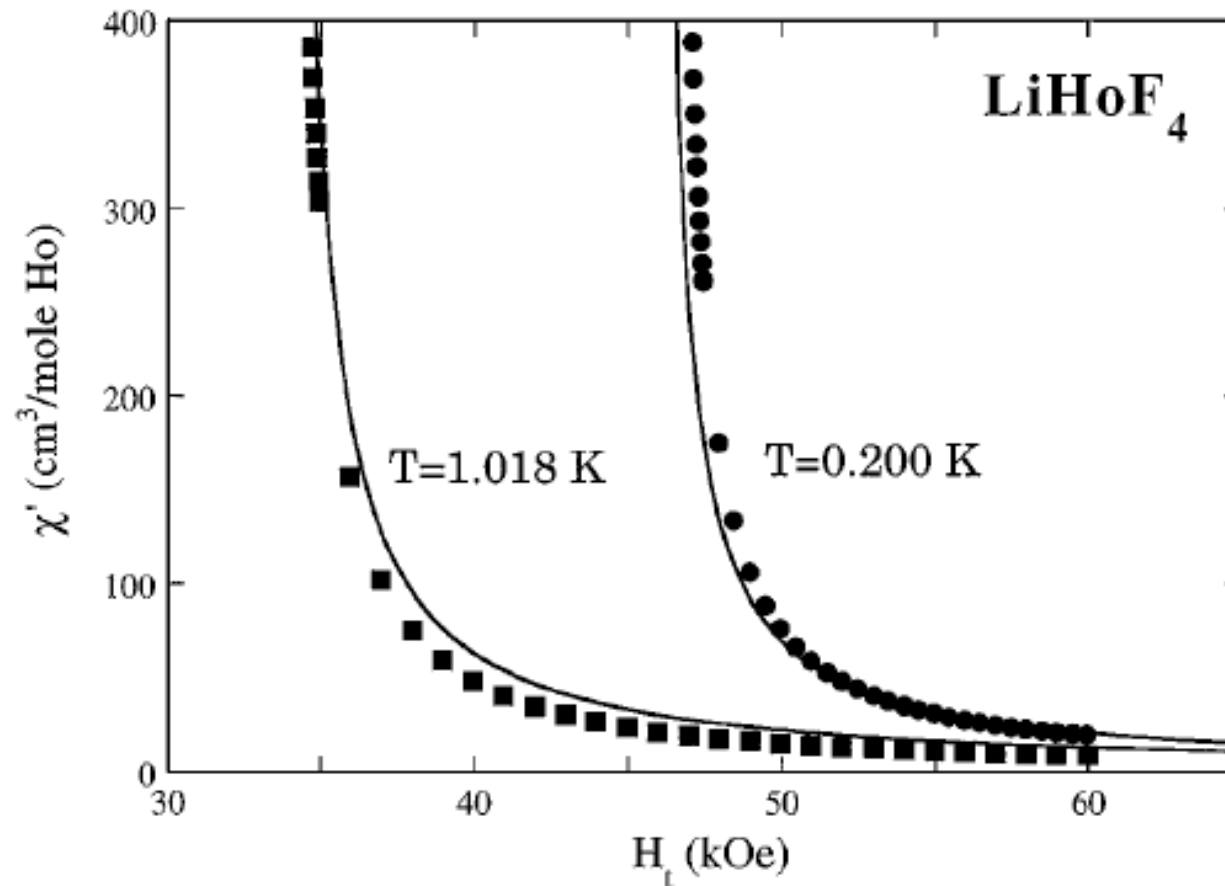
FIG. 4. Transverse field dependence of the susceptibility in the paramagnet for two temperatures. Solid line is a first principles calculation with parameters fixed by the fit to the phase boundary of Fig. 3.

Long-Range Ferromagnetism of Mn$_{12}$ Acetate Single-Molecule Magnets under a Transverse Magnetic Field

F. Luis,[1,*] J. Campo,[1] J. Gómez,[2] G. J. McIntyre,[3] J. Luzón,[1] and D. Ruiz-Molina[2]

[1]*Instituto de Ciencia de Materiales de Aragón, CSIC-Universidad de Zaragoza, 50009 Zaragoza, Spain*
[2]*Institut de Ciencia de Materials de Barcelona, Campus de la UAB, Bellaterra 08193, Spain*
[3]*Institut Laue Langevin, 6 rue Jules Horowitz, 38042 Grenoble, France*

We use neutron diffraction to probe the magnetization components of a crystal of Mn$_{12}$ single-molecule magnets. Each of these molecules behaves, at low temperatures, as a nanomagnet with spin $S = 10$ and strong anisotropy along the crystallographic c axis. The application of a magnetic field $H_\perp$ perpendicular to c induces quantum tunneling between opposite spin orientations, enabling the spins to attain thermal equilibrium. For $T \lesssim 0.9(1)$ K, this equilibrium state shows spontaneous magnetization, indicating the onset of ferromagnetism. These long-range magnetic correlations nearly disappear for $\mu_0 H_\perp \gtrsim 5.5$ T, possibly suggesting the existence of a quantum critical point.

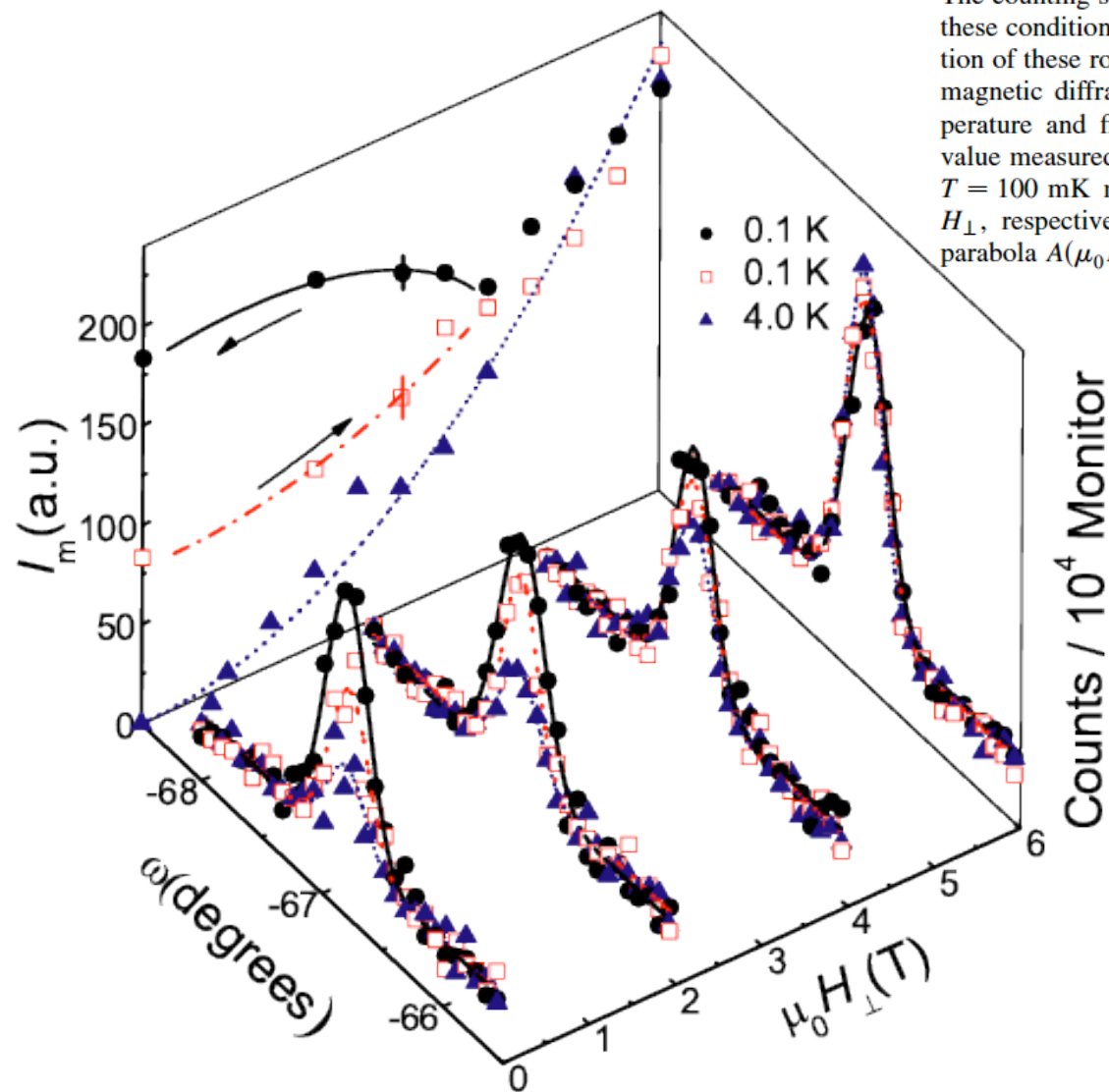Física de Bajas Temperaturas - Transiciones de Fase

FIG. 1 (color online). Rocking curves for the $(\bar{2}\,\bar{2}\,0)$ reflection measured at two different temperatures and four magnetic fields. The counting statistics are typical for such a small crystal under these conditions. The lines are Gaussian fits. Numerical integration of these rocking curves gives the diffracted intensity I. The magnetic diffraction intensities I_m were obtained at each temperature and field by subtracting from the total intensity the value measured at 4 K and $\mu_0 H_\perp = 0$. ▲, $T = 4$ K; □ and ●, $T = 100$ mK measured while increasing and then decreasing $H_\perp$, respectively. The dotted line is a least-squares fit to a parabola $A(\mu_0 H_\perp)^2$.
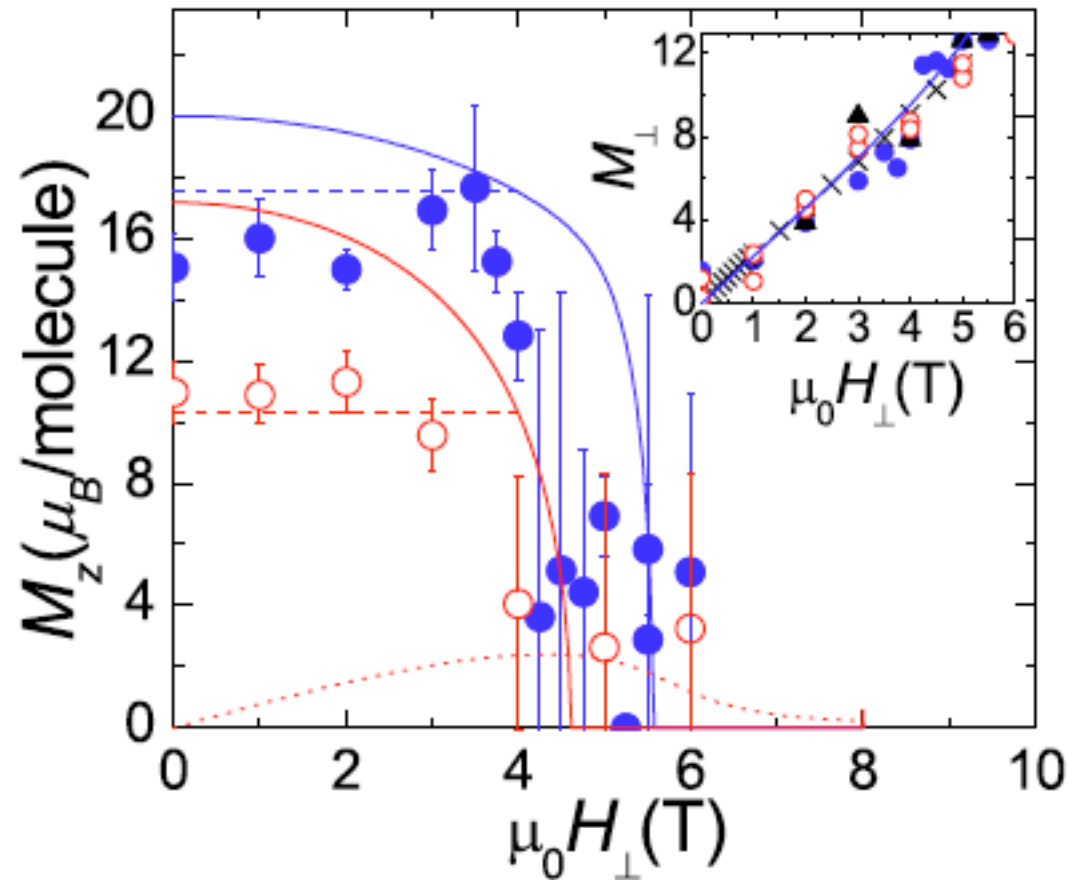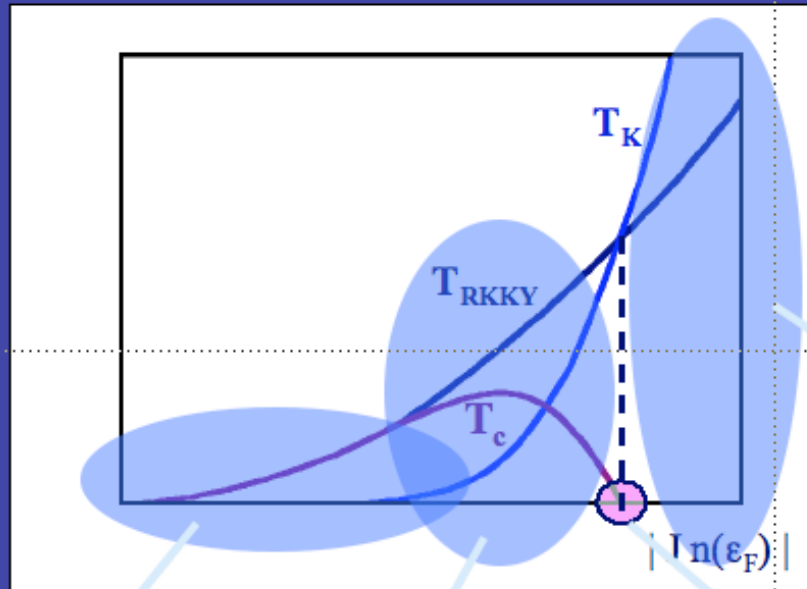
FIG. 2 (color online).   Longitudinal magnetization M_z of Mn_{12} acetate measured while decreasing the transverse magnetic field from 6 T. ● and ○ are for $T = 47$ and 600 mK, respectively.

Física de Bajas Temperaturas - Transiciones de Fase

Diagrama de Doniach

$$T_{RKKY} \propto \left(J\, n(\varepsilon_F) \right)^2$$

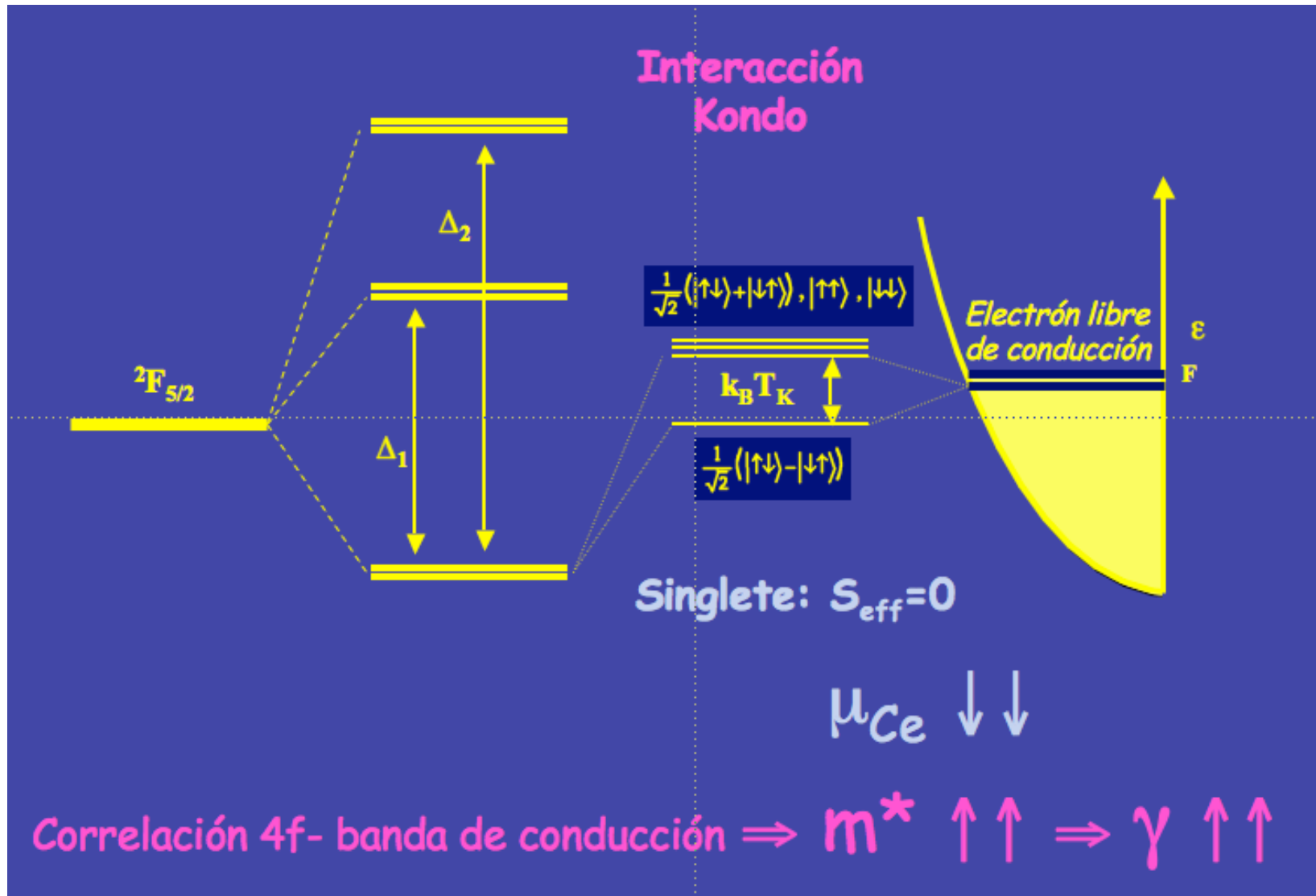$$T_K \propto e^{-\left(\frac{1}{|J|\, n(\varepsilon_F)} \right)}$$

$T_{RKKY} \gg T_K$

El sistema se ordena
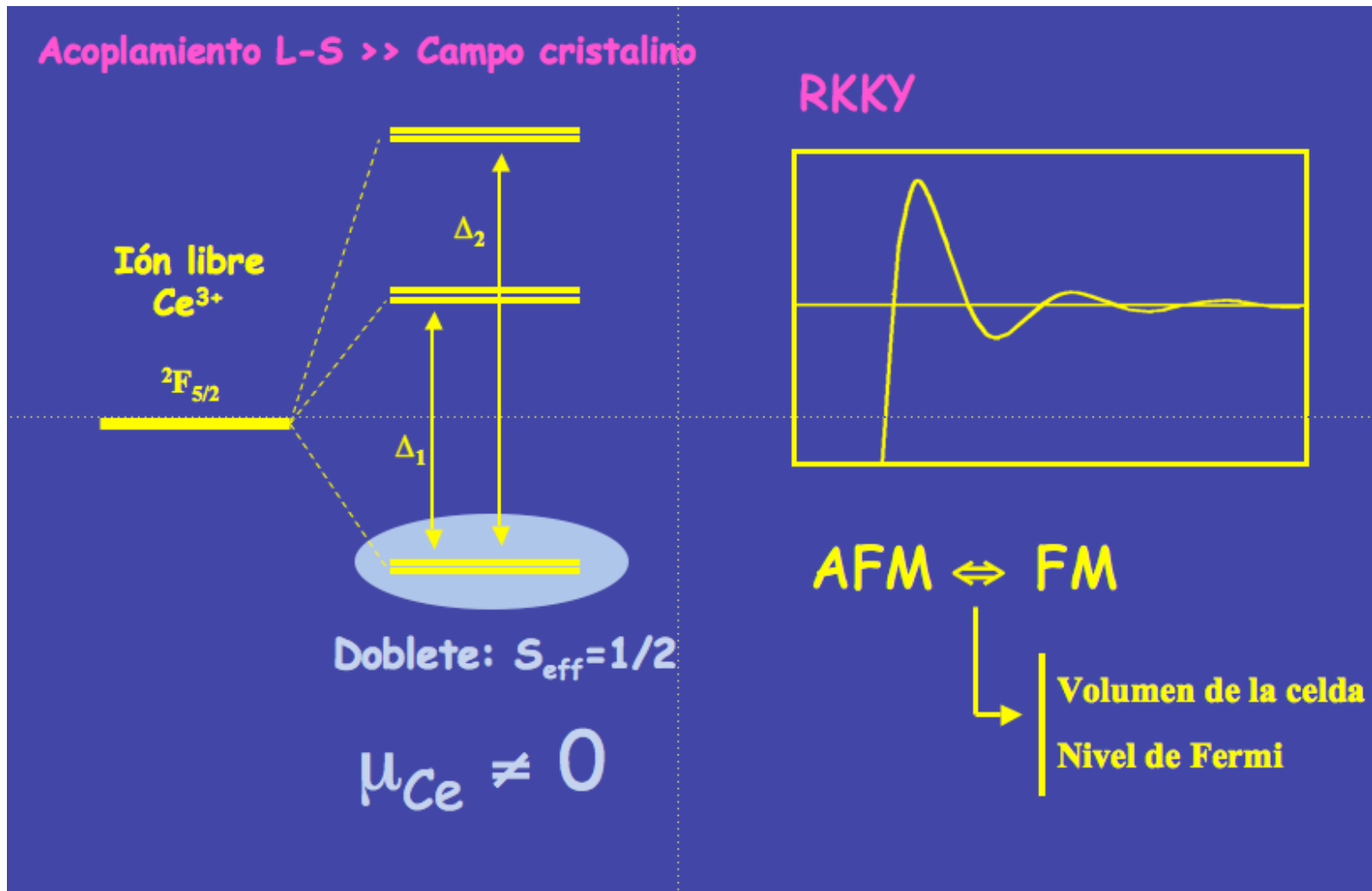
$T_{RKKY} \gtrsim T_K$

Momento magnético promedio reducido
El sistema se puede ordenar

$T_C \to 0$

Desaparición del magnetismo
Hibridación 4f-banda de conducción muy fuerte

$T_{RKKY} < T_K$

Estado fundamental no magnético

} NFL

Física de Bajas Temperaturas - Transiciones de Fase

Física de Bajas Temperaturas - Transiciones de Fase

Física de Bajas Temperaturas - Transiciones de Fase

# Quantum phase transitions in strongly correlated electron systems

Hilbert v. Löhneysen

Physikalisches Institut, Universität Karlsruhe, D-76128 Karlsruhe, Germany

A number of strongly correlated electron systems, notably heavy-fermion alloys, exhibit remarkable deviations from Fermi-liquid behavior at low temperatures. We focus on $CeCu_{6-x}Au_x$ and related alloys which have been studied most thoroughly. Non-Fermi-liquid behavior, i.e. unusual temperature dependencies of the specific heat, magnetic susceptibility, and electrical resistivity is found at the critical concentration where a quantum phase transition occurs from a nonmagnetic ground state (i.e. $CeCu_6$) to a magnetically ordered state ($x > 0.1$). This transition can also be tuned by external pressure, but tuning by an applied magnetic field leads to different behavior.
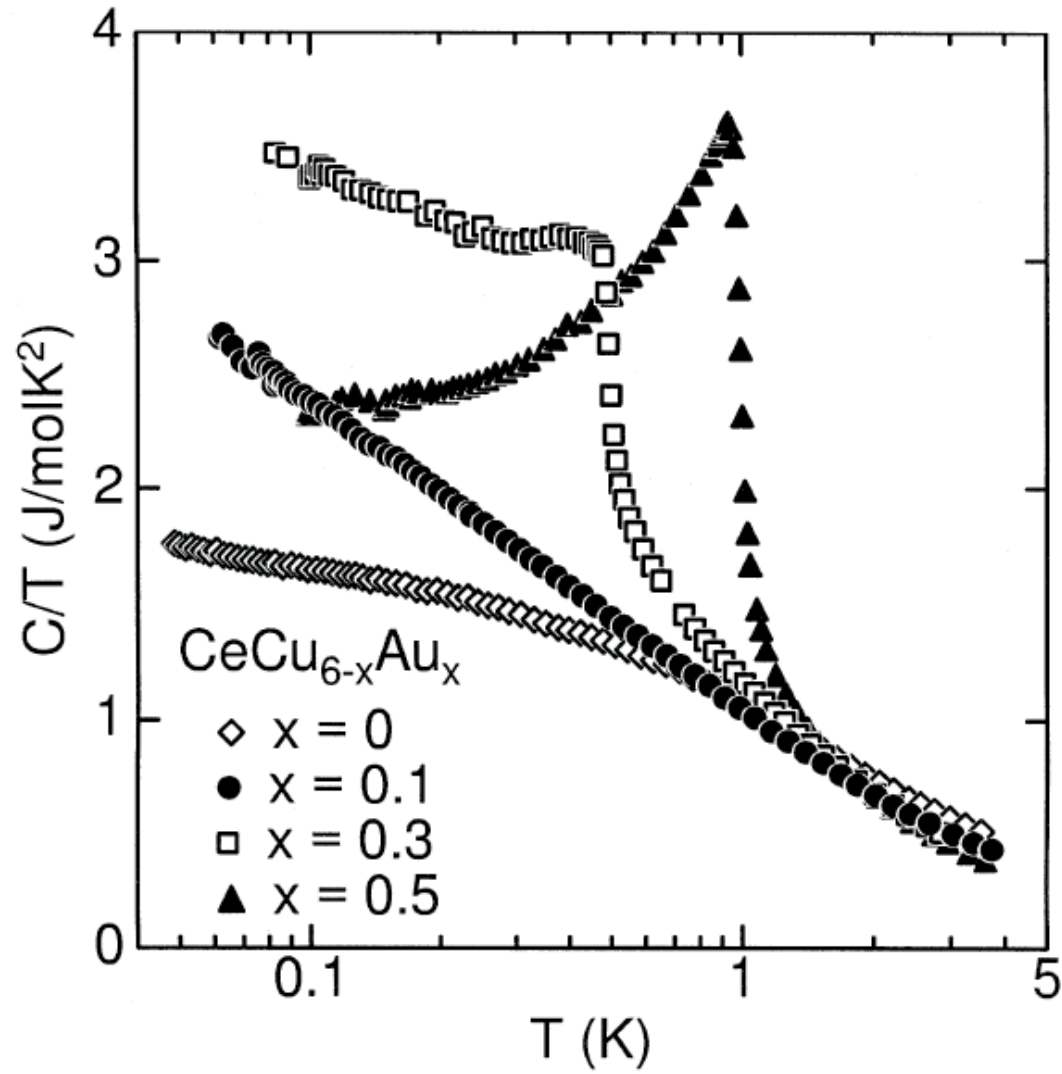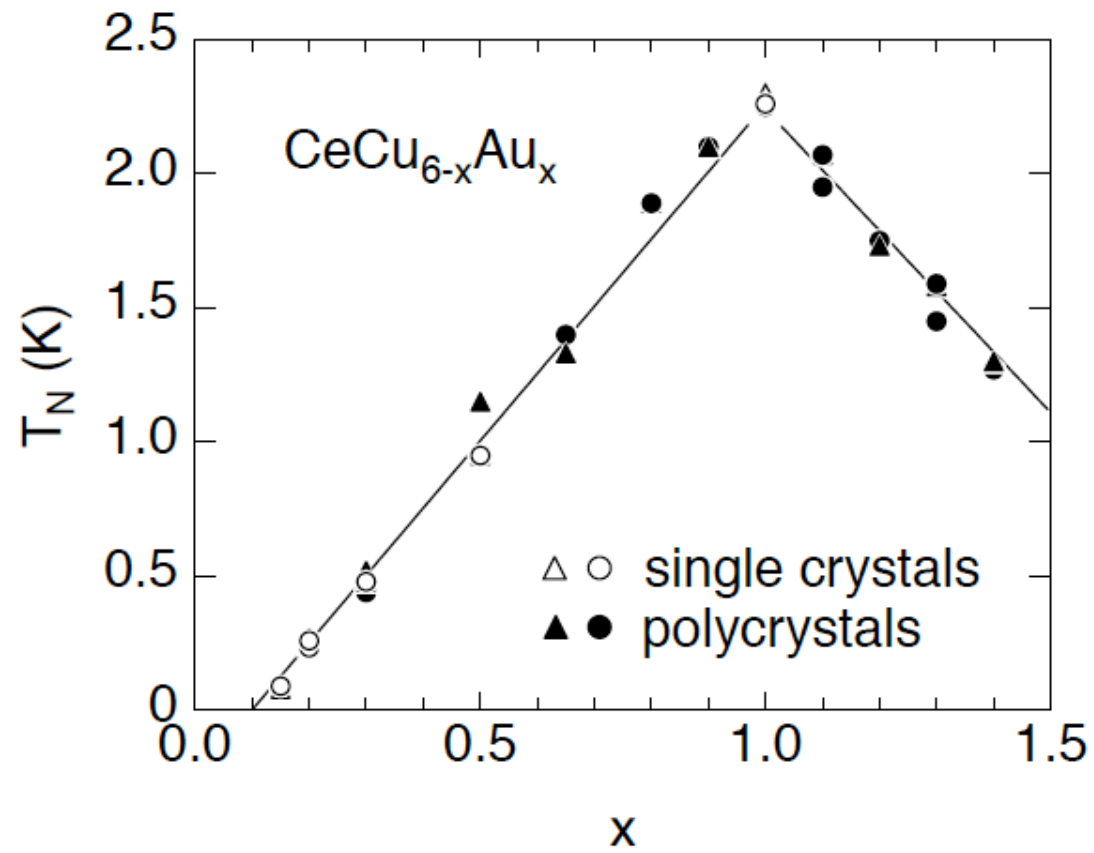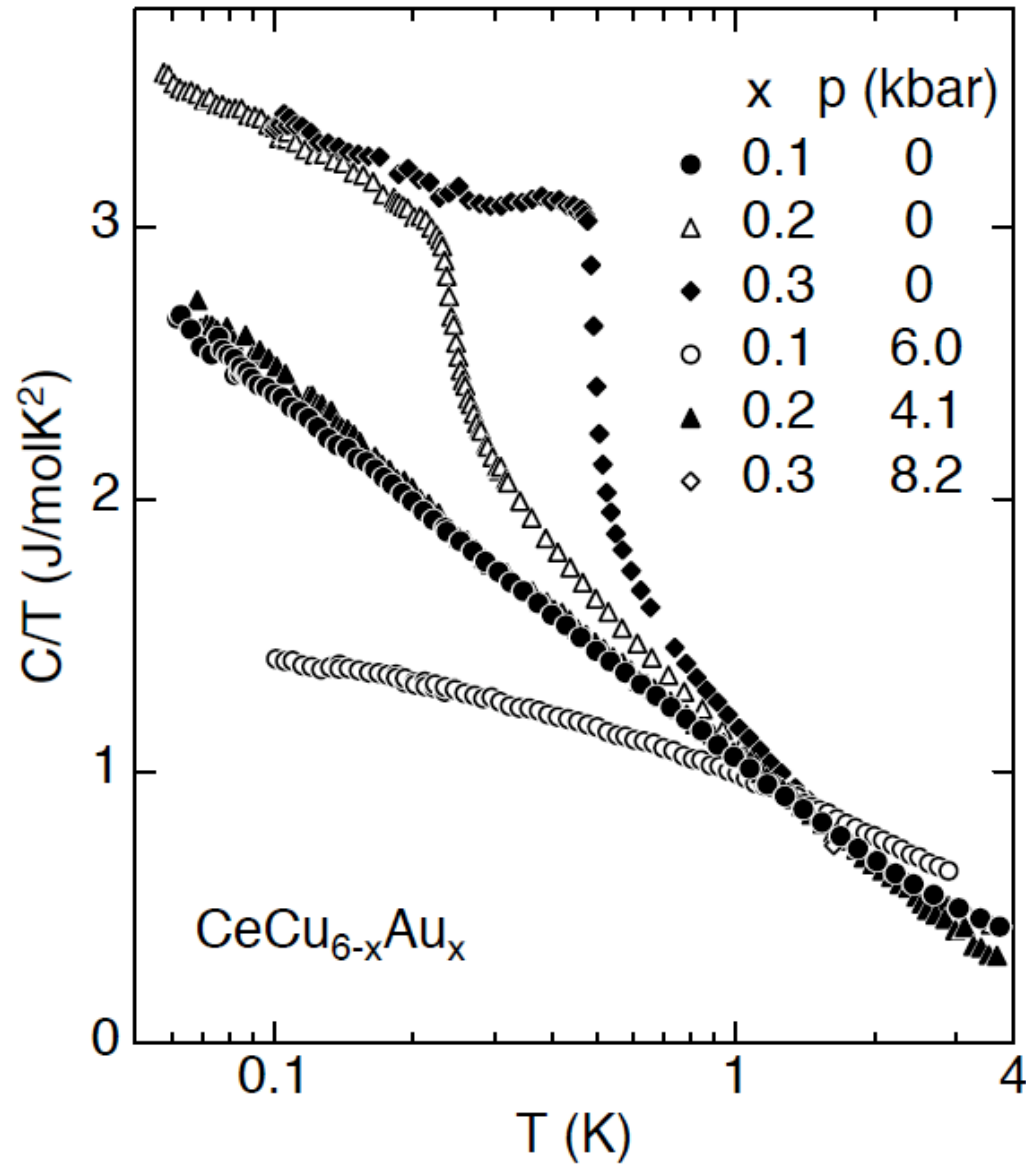
Magnetic ground state of CeNi$_{1-x}$Cu$_x$: A calorimetric investigation

N. Marcano, J. I. Espeso, J. C. Gómez Sal, and J. Rodríguez Fernández

Departamento de Ciencias de la Tierra y Física de la Materia Condensada, Facultad de Ciencias, Universidad de Cantabria
39005 Santander, Spain

J. Herrero-Albillos and F. Bartolomé

Instituto de Ciencia de Materiales de Aragón, CSIC Universidad de Zaragoza, 50009 Zaragoza, Spain

CeNi$_{1-x}$Cu$_x$ is a substitutional magnetic system where the interplay of the different magnetic interactions leads to the disappearance of the long-range magnetic order on the CeNi side. The existence of inhomogeneities (spin clusters or phase coexistence) has been previously detected by magnetization and muon spin relaxation (μSR) spectroscopy measurements. These inhomogeneities are always observed regardless of the different preparation methods and must, then, be considered as intrinsic. We present a detailed specific heat study in a large temperature range of 0.2 to 300 K. The analysis of these data, considering also previous neutron scattering, magnetic characterization, and μSR results, allows us to present a convenient description of the system as inhomogeneous on the nanometric scale. Two regimes are detected in the compositional range depending on the dominant Ruderman-Kittel-Kasuya-Yosida or Kondo interactions. We propose that the long-range magnetic order at low temperatures is achieved by a percolative process of magnetic clusters that become static below the freezing temperature T_f. In this scenario the existence of a quantum critical point at the magnetic-nonmagnetic crossover must be discarded. This situation should be considered as an example for other substitutional compounds with anomalous magnetic or superconducting properties.
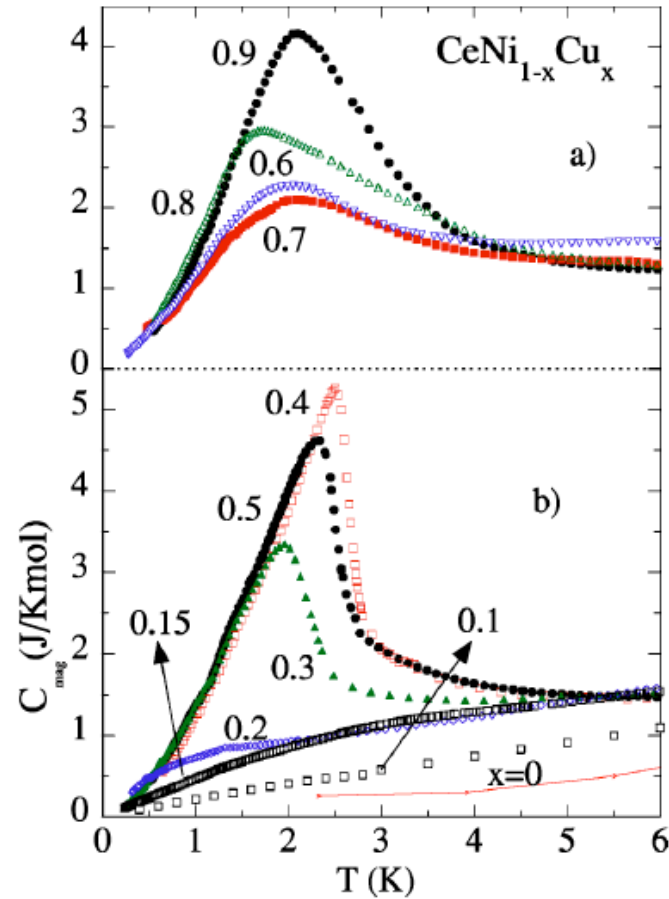
Física de Bajas Temperaturas - Transiciones de Fase

FIG. 5. C_{mag} versus temperature in the low-temperature regime plotted separately for the two composition regions defined: (a) 0.9 $\leqslant x \leqslant 0.6$ or region where the system evolves from AFM to FM ground state; (b) $x \leqslant 0.6$ or region where hybridization effects and disorder are predominant (for details see text).
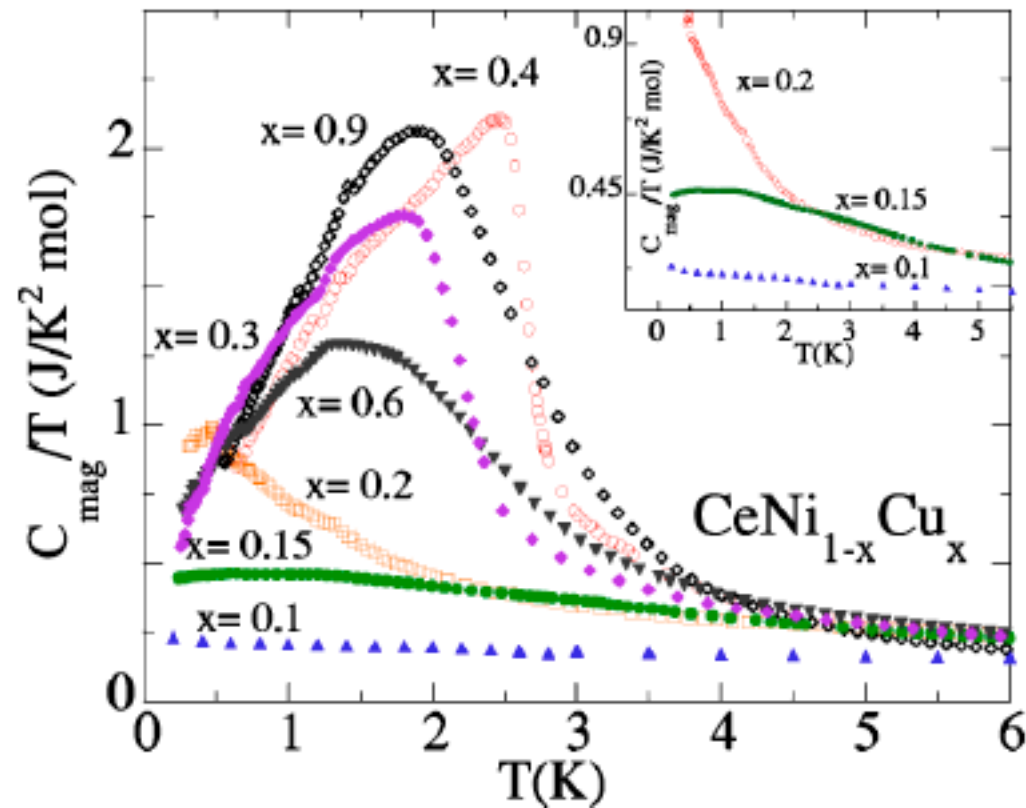
FIG. 6. C_{mag}/T vs T representation of the specific heat for $CeNi_{1-x}Cu_x$ in the compositions studied. The inset shows the variation for the compounds near the magnetic-nonmagnetic crossover $x=0.1$, 0.15, and 0.2.

studies by both macroscopic (ac and dc measurements[14]) and microscopic (μSR) techniques[13] in the compositions around $x=0.2$ revealed that the magnetic moments are not yet exhausted. However, long-range magnetic order, if it exists, cannot be detected by neutron diffraction (within the resolution of the available experiments) since we are dealing with very reduced values of the magnetic moment. Both experiments point toward some kind of short-range ordered states and reveal evidence of spin-glass arrangements even for the $x=0.1$ compound.[15] Thus, on the basis of all these results we have to discard an intrinsic electronic effect leading to a NFL or quantum phase transition around the $x=0.2$ compound. The divergence in C_{mag}/T could be related to the existence of a small anomaly at lower temperatures as was found at very low temperature in ac susceptibility measurements.[14]

Física de Bajas Temperaturas - Transiciones de Fase

How 'spin ice' freezes

J. Snyder*, J. S. Slusky†, R. J. Cava† & P. Schiffer*

* Department of Physics and Materials Research Institute,
Pennsylvania State University, University Park, Pennsylvania 16802, USA
† Department of Chemistry and Princeton Materials Institute,
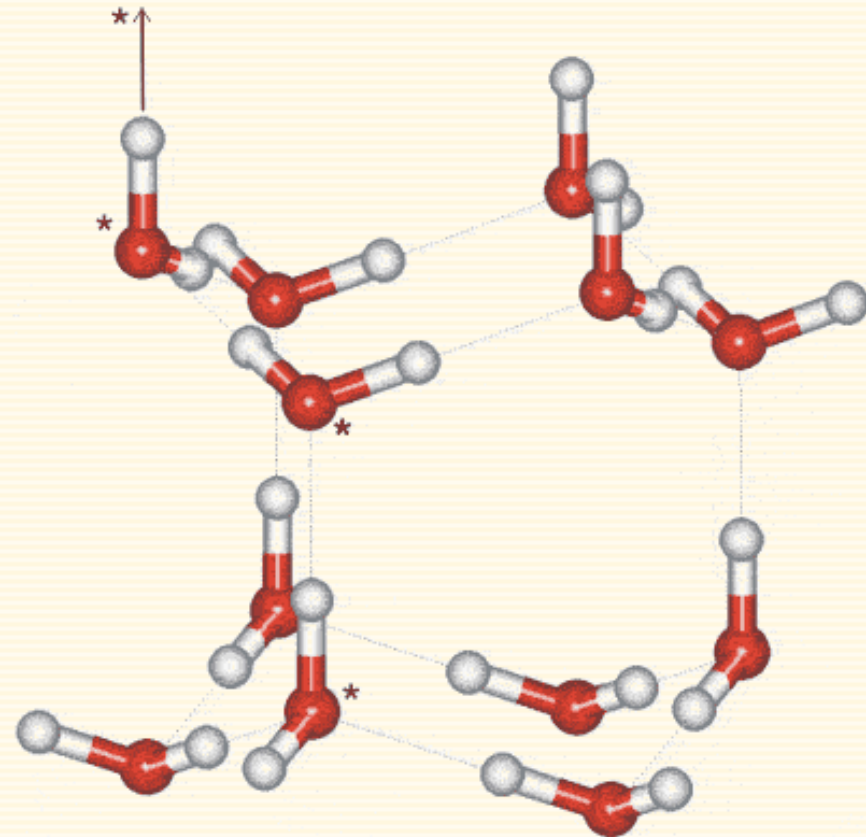Princeton University, Princeton, New Jersey 08540, USA

The large degeneracy of states resulting from the geometrical frustration of competing interactions is an essential ingredient of important problems in fields as diverse as magnetism[1], protein folding[2] and neural networks[3]. As first explained by Pauling[4], geometrical frustration of proton positions is also responsible for the unusual low-temperature thermodynamics of ice and its measured 'ground state' entropy[5]. Recent work has shown that the geometrical frustration of ice is mimicked by $Dy_2Ti_2O_7$, a site-ordered magnetic material in which the spins reside on a lattice of corner-sharing tetrahedra where they form an unusual magnetic ground state known as 'spin ice'[6–13]. Here we identify a cooperative
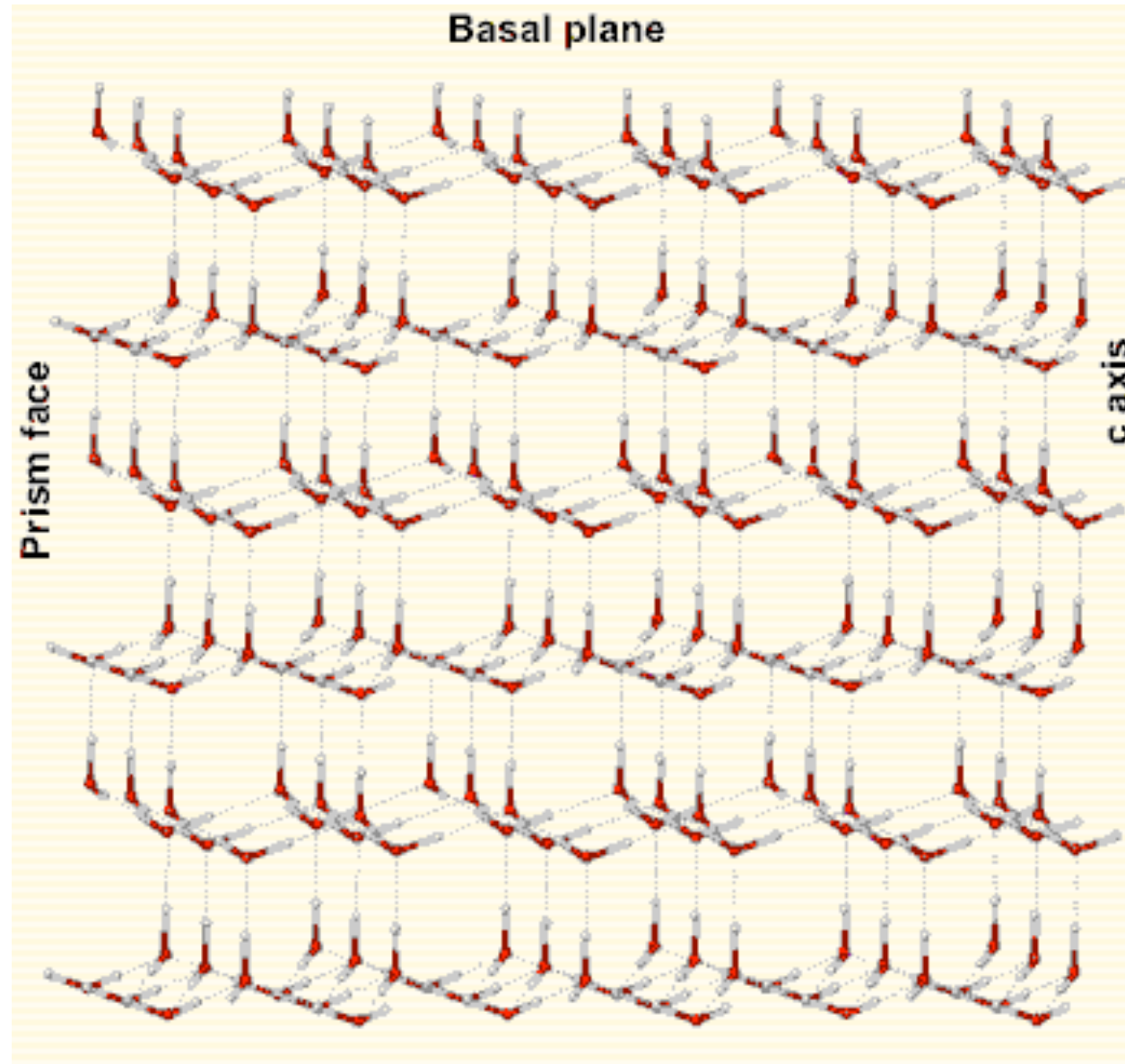
Hexagonal Ice (Ice Ih)

Hexagonal ice (ice Ih) is the form of all natural snow and ice on Earth (see Phase Diagram), as evidenced in the six-fold symmetry in ice crystals grown from water vapor (*i.e.* snow flakes).
Hexagonal ice (Space group P6$_3$/*mmc*, **194**;

Laue class symmetry 6/mmm; analogous to β-tridymite silica) possesses a fairly open low-density structure, where the packing efficiency is low (~1/3) compared with simple cubic (~1/2) or face centered cubic (~3/4) structures[1] (and in contrast to face centered cubic close packed solid hydrogen sulfide). The crystals may be thought of as consisting of sheets lying on top of each other. The basic structure consists of a hexameric box where planes consist of chair-form hexamers (the two horizontal planes, opposite) or boat-form hexamers (the three vertical planes, opposite). In this diagram the hydrogen bonding is shown ordered whereas in reality it is random.[2] The water molecules have a staggered arrangement of hydrogen bonding with respect to three of their neighbors, in the plane of the chair-form hexamers. The fourth neighbor (shown as vertical links opposite) has an eclipsed arrangement of hydrogen bonding.

Spin ice

Física de Bajas Temperaturas - Transiciones de Fase

Ice-seven (Ice VII) and Ice-ten (Ice X)

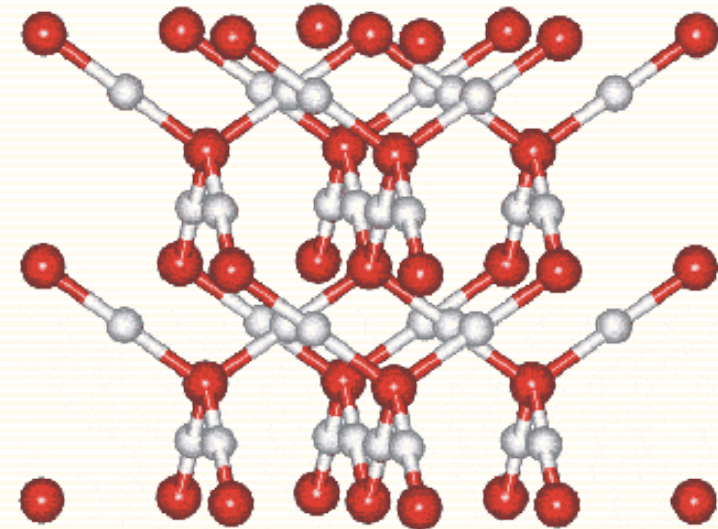Ice-seven (ice VII) is formed from liquid water above 3 GPa by lowering its temperature to ambient temperatures (see Phase Diagram). It can be obtained at low temperature and ambient pressure by decompressing (D_2O) ice-six below 95 K and is metastable over a wide range of pressure, transforming into LDA above 120 K [948].

Its unit cell, which forms cubic crystal (Pn3m, 224; Laue class symmetry m-3m). Ice VII consists of two interpenetrating cubic ice lattices with hydrogen bonds passing through the center of the water hexamers and no connecting hydrogen-bonds between lattices. It has a density of about 1.65 g cm^{-3} (at 2.5 GPa and 25°C [8]), which is less than twice the cubic ice density as the intra-network O····O distances are 8% longer (at 0.1 MPa) to allow for the interpenetration. The cubic crystal (shown opposite) has cell dimensions 3.3501 Å (a, b, c, 90º, 90º, 90º; D_2O, at 2.6 GPa and 22°C [361]) and contains two water molecules.

Física de Bajas Temperaturas - Transiciones de Fase
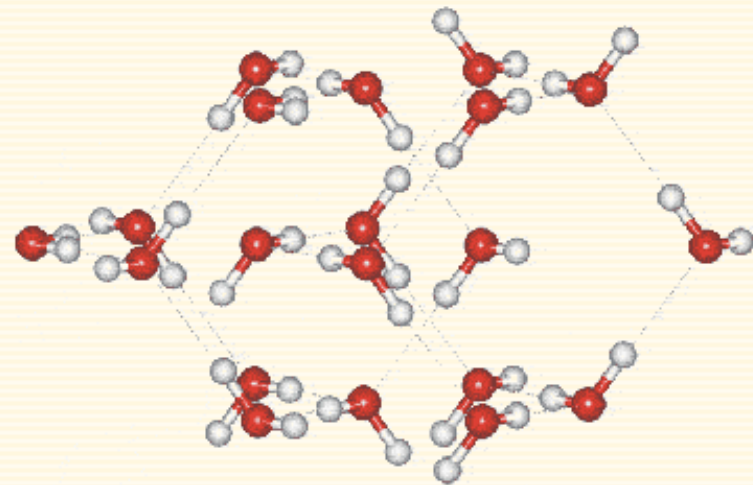
Ice-ten

As the pressure is raised and the O···O distance contracts, ice-seven appears to undergo a continuous transition into cubic ice-ten (ice X) (still Pn3m space group, a, b, c = 2.78 Å at 62 GPa, 300 K [719]) where the ice protons are equispaced (and equally bonded) between the oxygen atoms [391] in a molecular crystal. The oxygen atoms are arranged in a body-centered cubic arrangement (8 neighbors) and the hydrogen atoms in a body-centered truncated cubic arrangement (12 neighbors). The melting curve for ice-ten has been proposed at high temperatures (1000-2400 K) [612].
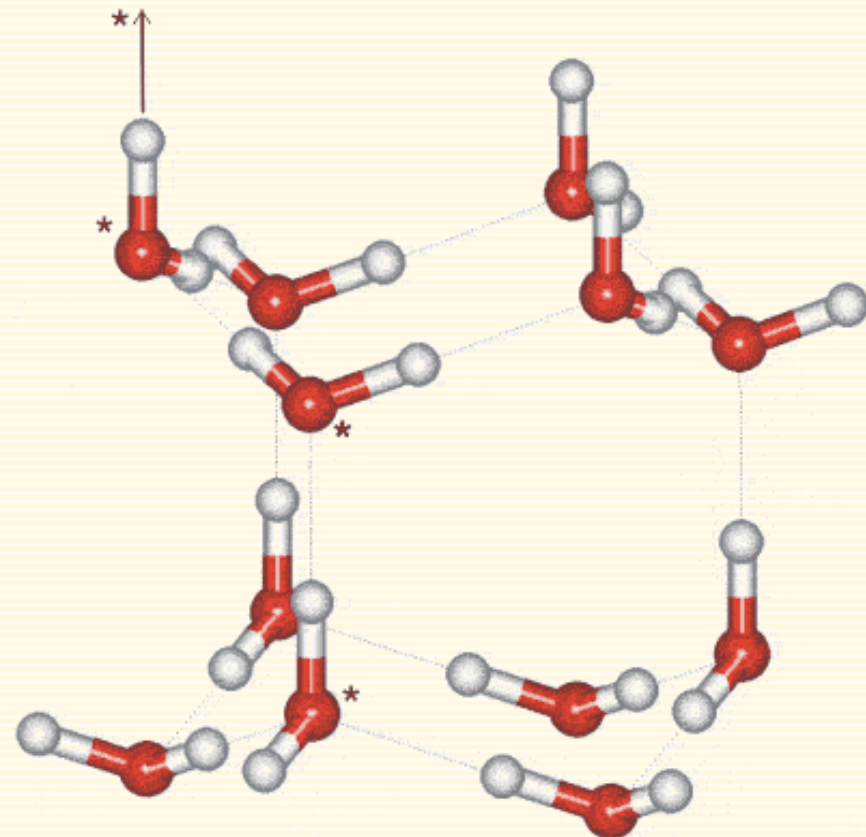
Hexagonal Ice (Ice Ih)

Hexagonal ice (ice Ih) is the form of all natural snow and ice on Earth (see Phase Diagram), as evidenced in the six-fold symmetry in ice crystals grown from water vapor (*i.e.* snow flakes).
Hexagonal ice (Space group $P6_3/mmc$, **194**;

Laue class symmetry 6/mmm; analogous to β-tridymite silica) possesses a fairly open low-density structure, where the packing efficiency is low (~1/3) compared with simple cubic (~1/2) or face centered cubic (~3/4) structures[1] (and in contrast to face centered cubic close packed solid hydrogen sulfide). The crystals may be thought of as consisting of sheets lying on top of each other. The basic structure consists of a hexameric box where planes consist of chair-form hexamers (the two horizontal planes, opposite) or boat-form hexamers (the three vertical planes, opposite). In this diagram the hydrogen bonding is shown ordered whereas in reality it is random.[2] The water molecules have a staggered arrangement of hydrogen bonding with respect to three of their neighbors, in the plane of the chair-form hexamers. The fourth neighbor (shown as vertical links opposite) has an eclipsed arrangement of hydrogen bonding.
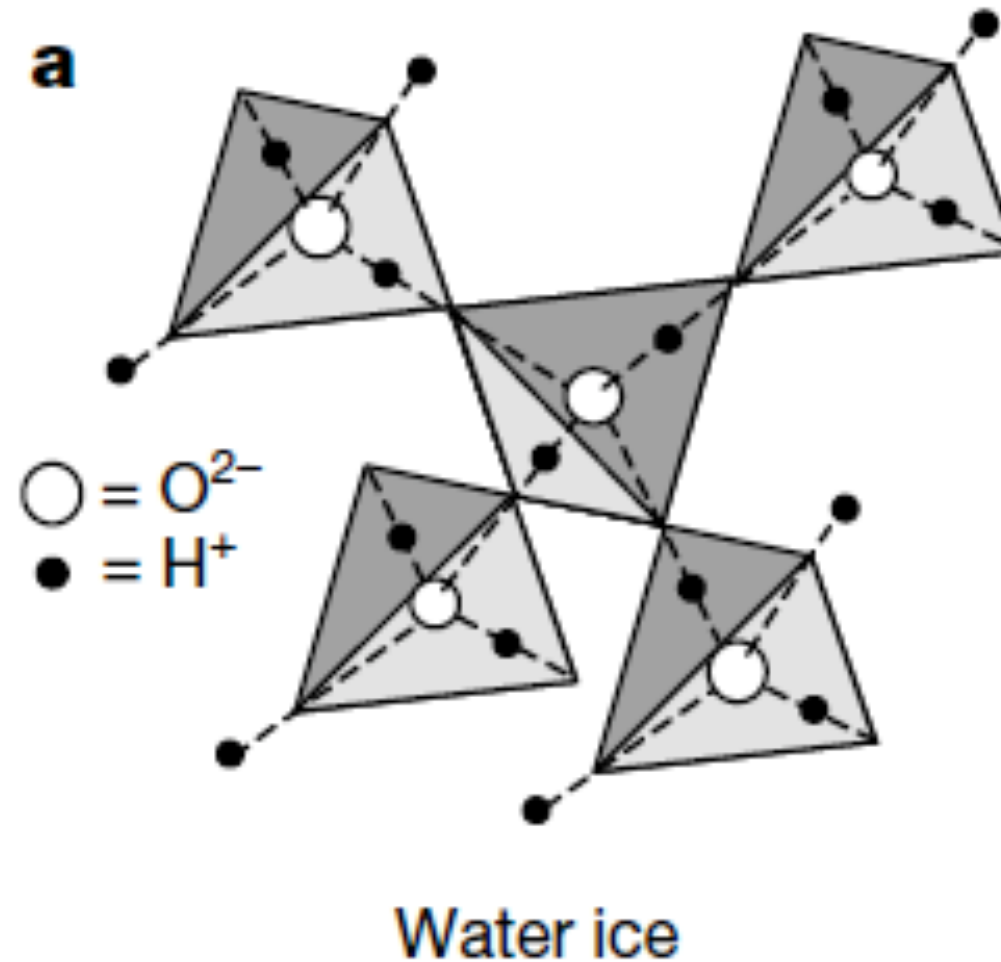
Física de Bajas Temperaturas - Transiciones de Fase

Water ice

Figure 1 Schematic representation of frustration in water ice and spin ice. **a**, In water ice, each hydrogen ion is close to one or the other of its two oxygen neighbours, and each oxygen must have two hydrogen ions closer to it than to its neighbouring oxygen ions. **b**, In
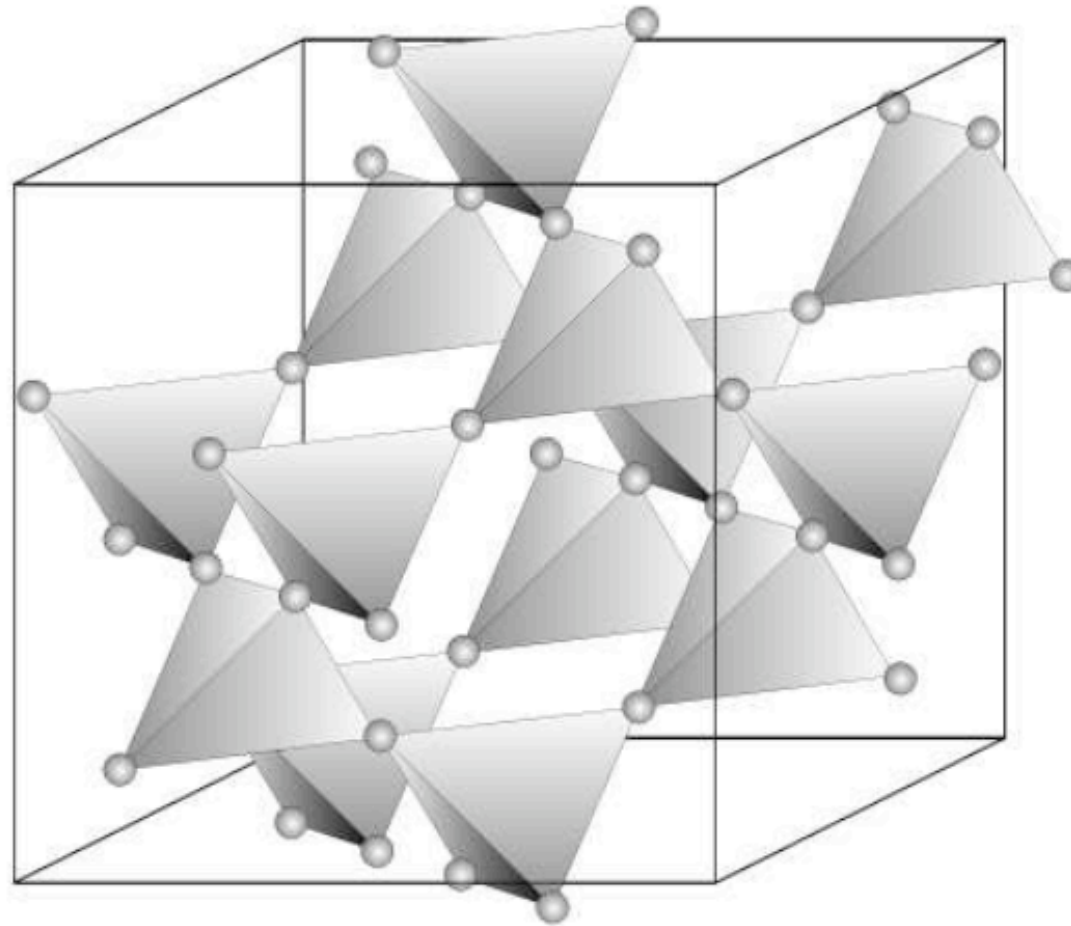
Fig.1   Pyrochlore lattice
This lattice consists of corner-shared tetrahedron. Atoms reside on the vertices of
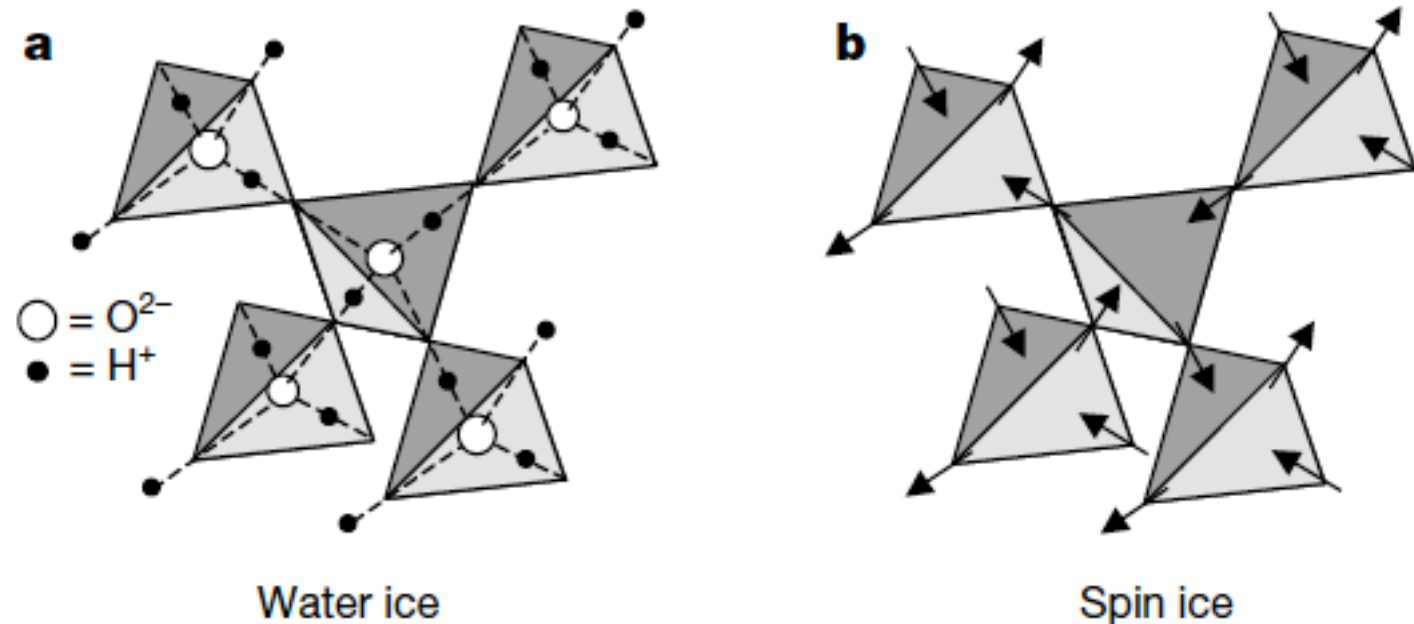each tetrahedron.

Water ice

Spin ice

Figure 1 Schematic representation of frustration in water ice and spin ice. **a**, In water ice, each hydrogen ion is close to one or the other of its two oxygen neighbours, and each oxygen must have two hydrogen ions closer to it than to its neighbouring oxygen ions. **b**, In spin ice, the spins point either directly toward or away from the centres of the tetrahedra, and each tetrahedron is constrained to have two spins pointing in and two pointing out.
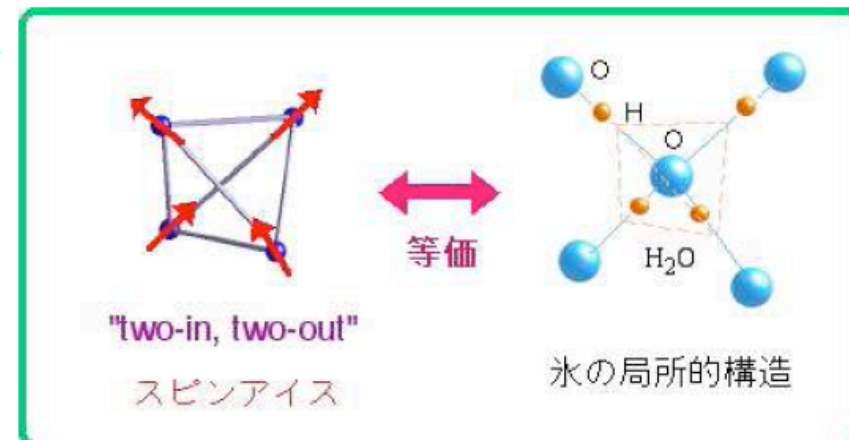
- $Ho_2Ti_2O_7$ (and $Dy_2Ti_2O_7$) are pyrochlore Ising magnets which do not order at $T \ll \Theta_W$ Bramwell+Harris

- Residual low-T entropy: Pauling entropy for water ice $\mathcal{S}_0 = (1/2)\ln(3/2)$ Ramirez *et al.*:

Física de Bajas Temperaturas - Transiciones de Fase
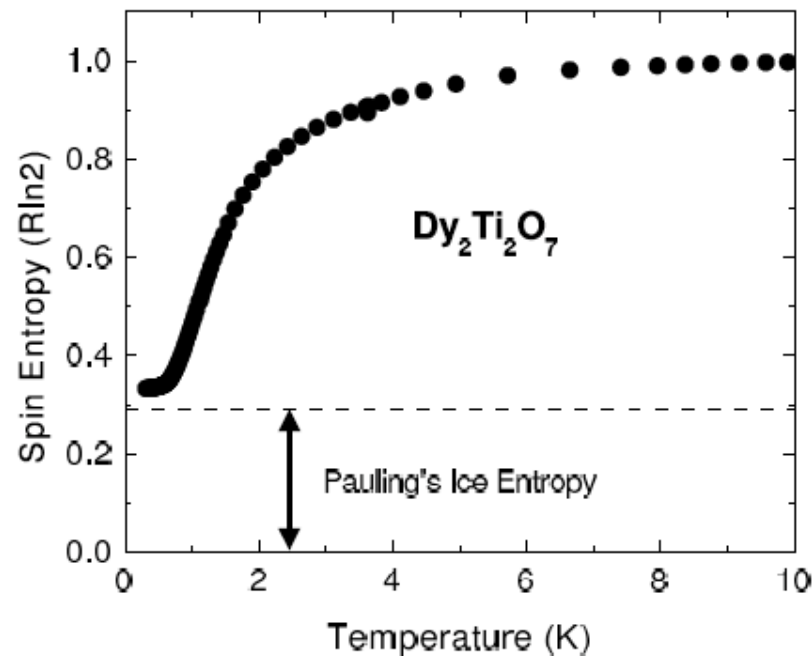
Spin ice and the ice rules

$$\mathcal{H} = -E \sum_i \left(\hat{\mathbf{d}}_{\kappa(i)} \cdot \mathbf{S}_i \right)^2 + J \sum_{\langle ij \rangle} \mathbf{S}_i \cdot \mathbf{S}_j = -(J/3) \sum_{\langle ij \rangle} \sigma_i \sigma_j$$

- Spins, $\mathbf{S}_i$, are forced to point along local [111] axes, $\hat{\mathbf{d}}_{\kappa(i)}$
  $\Rightarrow$ anisotropy, E, generates Ising pseudospins: $\mathbf{S}_i = \sigma_i \hat{\mathbf{d}}_{\kappa(i)}$

- there are four sublattices, κ, with $\hat{\mathbf{d}}_\kappa \cdot \hat{\mathbf{d}}_{\kappa'} = -1/3$
  $\Rightarrow J$ for pseudospins changes sign!

- Ground states have $\sum \sigma_i = 0$ for each tetrahedron

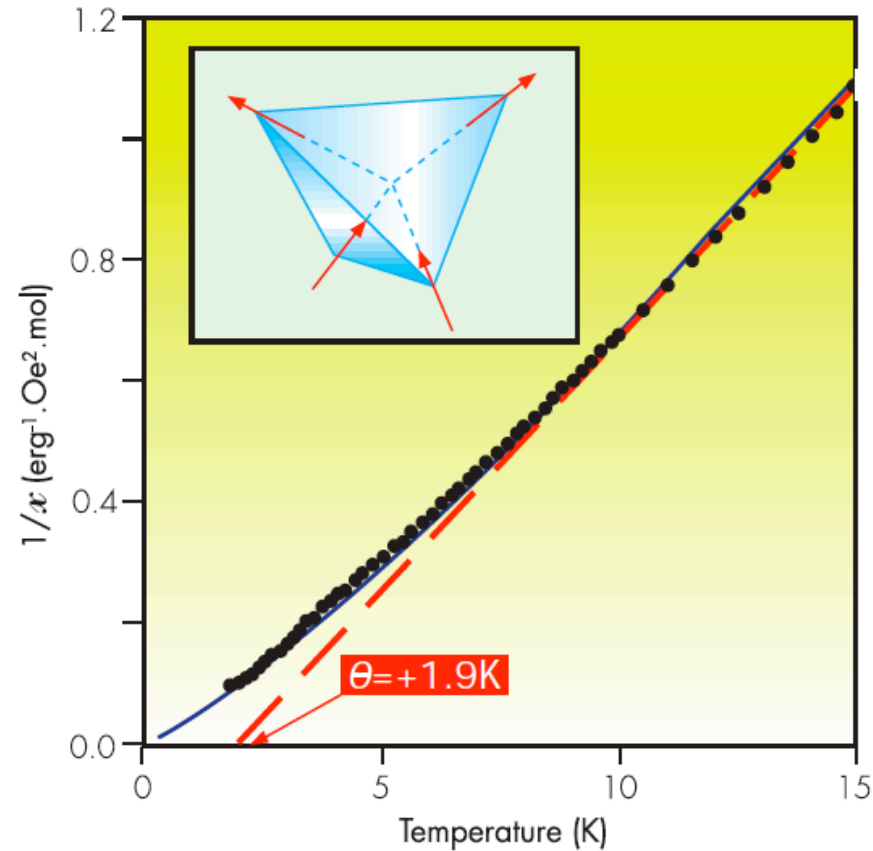- These are the two-in two-out states (Bernal-Fowler ice rules)

"two-in, two-out"

スピンアイス

等価

H₂O

氷の局所的構造

Spin ice

Física de Bajas Temperaturas - Transiciones de Fase

Figure F14.1. The inverse susceptibility of $Ho_2Ti_2O_7$ with a Monte Carlo simulation of the spin ice model shown as a blue line, and the standard Curie-Weiss law as a red line. The inset shows the ground state of a single tetrahedron of spins with ferromagnetic coupling and <111> anisotropy.
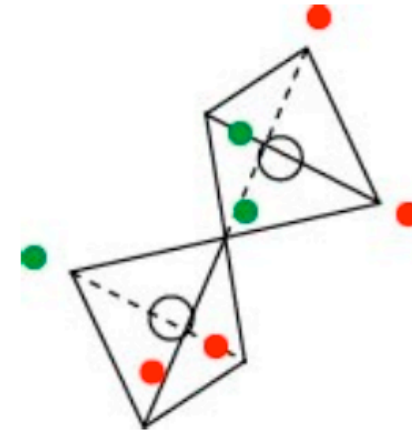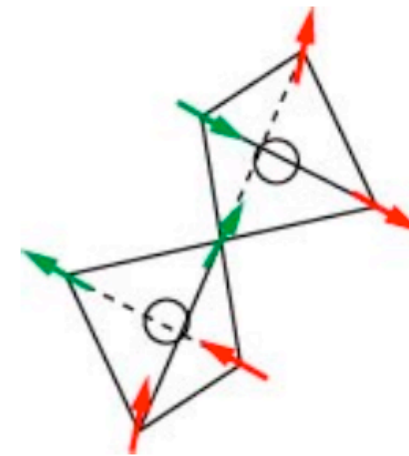

Fig.3   Proton ordering in water ice

Spin configuration in a spin ice